# 研究成果の刊行に関する一覧表

## 書籍

| 著者氏名 | 論文タイトル名 | 書籍全体の編集者名 | 書　籍　名 | 出版社名 | 出版地 | 出版年 | ページ |
|---|---|---|---|---|---|---|---|
| 久保寺隆行, 仁科一隆, 横田隆徳 | 神経筋疾患のRNAi治療の展望 | 鈴木則宏<br>祖父江　元<br>荒木信夫<br>宇川義一<br>川原信隆 | Annual Review<br>神経2011 | 中外医学社 | 日本 | 2011 | 42-52 |

## 雑誌

| 発表者氏名 | 論文タイトル名 | 発表誌名 | 巻号 | ページ | 出版年 |
|---|---|---|---|---|---|
| Uno Y, Piao W, Nishina K, Miyata K, Mizusawa H, Yokota T | HDL facilitates in vivo delivery of a-tocopherol-conjugated siRNA to the brain | Hum Gene Ther | EPub | | 2011 |
| Mayra A, Tomimitsu H, Kubodera T, Kobayashi M, Piao W, Sunaga F, Hirai Y, Shimada T, Mizusawa H, Yokota T | Intraperitoneal AAV9-shRNA inhibits target expression in neonatal skeletal and cardiac muscles | Biochem Bioph Res Commun | 405 | 204-209 | 2011 |
| Kubodera T, Yamada H, Anzai M, Ohira S, Yokota S, HiraiY, Mochizuki H, Shimada T, Mitani T, Mizusawa H, Yokota T | In Vivo application of an RNAi strategy for the selective suppression of a mutant allele | Hum Gene Ther | 22 | 27-34 | 2011 |

| 発表者氏名 | 論文タイトル名 | 発表誌名 | 巻号 | ページ | 出版年 |
|---|---|---|---|---|---|
| Okabayashi S, Kimura N | LGI3 interacts with flotillin-1 to mediate APP trafficking and exosome formation | Neuroreport | 21 | 606-610 | 2010 |
| Oikawa N, Kimura N, Yanagisawa K. | Alzheimer-type tau pathology in advanced aged nonhuman primate brains harboring substantial amyloid depositio | Brain Res | 1315 | 137-149 | 2010 |

# Ⅳ. 研究成果の刊行物・別刷

HUMAN GENE THERAPY 00:1–9 (XXXXX 2011)

DOI: 10.1089/hum.2010.083

# High-Density Lipoprotein Facilitates *In Vivo* Delivery of α-Tocopherol–Conjugated Short-Interfering RNA to the Brain

Yoshitaka Uno,[1] Wenying Piao,[1] Kanjiro Miyata,[2] Kazutaka Nishina,[1] Hidehiro Mizusawa,[1] and Takanori Yokota[1]

**Abstract**

We originally reported the use of vitamin E (α-tocopherol) as an *in vivo* vector of short-interfering RNA (siRNA) to the liver. Here, we apply our strategy to the brain. By combining high-density lipoprotein (HDL) as a second carrier with α-tocopherol–conjugated siRNA (Toc-siRNA) in the brain, we achieved dramatic improvement of siRNA delivery to neurons. After direct intracerebroventricular (ICV) infusion of Toc-siRNA/HDL for 7 days, extensive and specific knock-down of a target gene, β-site amyloid precursor protein cleaving enzyme 1 (*BACE1*), was observed in both mRNA and protein levels, especially in the cerebral cortex and hippocampus. This new delivery method achieved a much more prominent down-regulation effect than conventional silencing methods of the brain gene, i.e., ICV infusion of nonconjugated siRNA or oligonucleotides. With only 3 nmol Toc-siRNA with HDL, BACE1 mRNA in the parietal cortex could be reduced by ~70%. We suppose that this dramatic improvement of siRNA delivery to the brain is due to the use of lipoprotein receptor–mediated endocytosis because the silencing efficiency was significantly increased by binding of Toc-siRNA to the lipoprotein, and in contrast, was clearly decreased in lipoprotein-receptor knockout mice. These results suggest exogenous siRNA could be used clinically for otherwise incurable neurological diseases.

## Introduction

THE POSSIBLE THERAPEUTIC APPLICATIONS of short-interfering RNA (siRNA) cover a wide spectrum of disorders, including cancer, infectious diseases, and inherited diseases. There has been much interest in the clinical applications of siRNA to neurological diseases such as Alzheimer's disease (AD), Huntington's disease, Parkinson's disease, and amyotrophic lateral sclerosis. However, delivery of siRNA to the brain has not been well established.

For *in vivo* delivery of siRNA, viral vectors and high-pressure, high-volume intravenous injection methods have been described. However, these approaches have limitations in clinical practice due to their side effects. Much progress has been reported on intravenous administration of siRNA to the liver using cationic liposomes, nanoparticles, and cell-penetrating peptides (Zimmermann *et al.*, 2006; Moschos *et al.*, 2007; Rozema *et al.*, 2007; Wolfrum *et al.*, 2007; Akinc *et al.*, 2008, 2009; Gao *et al.*, 2009). Ligand conjugation for receptor-mediated uptake system is also expected to be another possible delivery method *in vivo* (Kumar *et al.*, 2007).

We recently published a report of efficient systemic delivery of siRNA to the liver by using conjugation with α-tocopherol (Nishina *et al.*, 2008). We expected that the most effective *in vivo* carrier would be a molecule that is essential for target tissue cells but cannot be synthesized within the cells. Vitamins fit these requirements well, and the least toxic vitamin, even at high doses, is vitamin E (Kappus and Diplock, 1992). α-Tocopherol is a lipophilic natural molecule and has physiological pathways from blood to the brain as well as to the liver. Orally ingested α-tocopherol is absorbed at the ileum, incorporated into chylomicrons, and transferred to very-low-density lipoprotein (VLDL) in the liver by α-tocopherol transfer protein (αTTP). VLDL containing α-tocopherol is metabolized to low-density lipoprotein (LDL) and HDL, which supply α-tocopherol to all tissue cells via their respective lipoprotein receptors (Rigotti, 2007). The delivery pathway of α-tocopherol to the brain has not been

[1]Department of Neurology and Neurological Science, Graduate School, Tokyo Medical and Dental University, Bunkyo-ku, Tokyo 113-0034, Japan.
[2]Division of Clinical Biotechnology, Center for Disease Biology and Integrative Medicine, Graduate School of Medicine, The University of Tokyo, Bunkyo-ku, Tokyo 113-0034, Japan.

well investigated. Brain endothelial cells have a receptor-mediated uptake system of α-tocopherol from α-tocopherol–containing HDL and LDL through each receptor (Goti *et al.*, 2002; Mardones *et al.*, 2002; Qian *et al.*, 2005). After α-tocopherol enters the brain, αTTP may have an important role in supplying α-tocopherol to neurons and glial cells. We and others showed that α-tocopherol in the brain was almost depleted in $\alpha TTP^{-/-}$ mice and was markedly decreased even in $\alpha TTP^{-/-}$ mice fed an α-tocopherol–rich diet resulting in increased serum α-tocopherol (Yokota *et al.*, 2001; Gohil *et al.*, 2008). αTTP is expressed in astrocytes (Hosomi *et al.*, 1998), and cholesterol, as a major lipid, is transferred to neurons and glial cells from astrocytes by HDL-like particles synthesized in astrocytes (Pfrieger, 2003; Vance *et al.*, 2005; Herz and Chen, 2006). We postulated that α-tocopherol could be delivered to neurons and glial cells by HDL-like particles in the brain. Although serum HDL and brain HDL-like particles are different in their composition and origin, their size and density are similar and both supply lipids through lipoprotein receptors with ApoE as a ligand (Vance *et al.*, 2005). Therefore, we attempted to use serum HDL as a carrier vector for α-tocopherol–conjugated siRNA to neurons and glial cells with delivery by direct ICV infusion.

## Materials and Methods

### *siRNAs*

α-Tocopherol–conjugated and Cy3-labeled siRNAs were synthesized by Hokkaido System Science (Sapporo, Japan). The sequences for the sense and antisense strands of siBACE are as follows: siBACE sense, 5′-GAAcCuAuGCGAuGCGA AuGUUUAU*A*C-3′; antisense, 5′-guauaaACAUuCGCAuC GCAUAgGUuC*U*U-3′. 2′-*O*-methyl–modified nucleotides are in lower case, and phosphorothioate linkages are represented by asterisks. α-Tocopherol and Cy3 fluorophore were covalently bound to the 5′-end of antisense and sense strands, respectively. siRNA duplexes were generated by annealing equimolar amounts of complementary sense and antisense strands.

### In vitro *siRNA transfection assay*

Neuro2a cells were transfected with each siRNA at 10 n*M* with Lipofectamine RNAiMAX, as described by the vendor (Invitrogen, Carlsbad, CA). For quantitative real-time polymerase chain reaction (qRT-PCR), total RNA was extracted and 2 μg of RNA was reverse-transcribed with Superscript III kit (Invitrogen). qRT-PCR was performed using the LightCycler 480 Probes Master and LightCycler 480 II (Roche Diagnostics, Mannheim, Germany) according to the manufacturer's instructions. Primers for mouse BACE1 and glyceraldehyde-3-phosphate dehydrogenase (GAPDH) mRNAs were designed by Applied Biosystems (Foster City, CA).

For Western blot analysis, transfected cells were harvested 48 hr post transfection. Cell pellets were purified for cytosolic fraction with NE-PER nuclear and cytoplasmic extraction reagents (Thermo Fisher Scientific, Waltham, MA). Samples were separated by 10% denaturing polyacrylamide gel electrophoresis (PAGE) and transferred onto polyvinylidene difluoride membranes. Blots were probed with a rabbit antibody against BACE1 (1:500, AB5832; Millipore, Billerica, MA) and confirmed with a mouse antibody against β-tubulin (1:2000, MAB1637; Chemicon, Temecula, CA). Blots were incubated with anti-rabbit or anti-mouse secondary antibodies (1:1000) tagged with horseradish peroxidase. Blots were visualized with SuperSignal West Femto Maximum Sensitivity Substrate (Thermo Fisher Scientific) and analyzed by a ChemiDoc system (Bio-Rad, Hercules, CA).

### *HDL collection*

The HDL fraction was prepared with sequential ultracentrifugation by a method described previously (Hatch and Lees, 1968). In brief, one volume of mouse serum and a half volume of density 1.182 solution was mixed and centrifuged for 3.5 hr at 450,000 × *g* at 16°C. A half volume of density 1.478 solution was then added to one volume of the bottom layer. The tubes were mixed and centrifuged for 4 hr, 50 min at 450,000 × *g* at 16°C. The top fraction containing HDL was used in the experiments.

### *HDL labeling with dipyrromethene boron difluoride*

To prepare dipyrromethene boron difluoride (BODIPY) working solution, cholesteryl BODIPY 542/563 C11 powder (Invitrogen) was dissolved in dimethyl sulfoxide at a concentration of 0.5 μg/ml. The BODIPY working solution and HDL fraction were mixed at a volume ratio of 1:5 and vortexed before use.

### In vitro *LDL receptor overexpression study*

HEK293T cells were grown in four-chamber slides ($1 \times 10^5$ cells/well) and transfected using Lipofectamine 2000 (Invitrogen) according to the manufacturer's protocol. Briefly, 600 ng of mouse LDL receptor (LDLR; cDNA clone MGC:62289) expressing plasmid (Origene, Rockville, MD) and 60 ng pEGFP (Clontech, Mountain View, CA) or reporter plasmid alone were mixed with 1 μl of Lipofectamine 2000 and added to each well. Following 24 hr of incubation, wells were gently washed three times with Dulbecco's modified Eagle medium (DMEM), then BODIPY-labeled HDL containing DMEM (1:30 volume ratio) was added to each well and the cells were further incubated for 3 hr. After incubation, cells were fixed with 4% paraformaldehyde and nuclei were counterstained with 4′,6-diamidino-2-phenylindole.

For Western blot analysis, cells were harvested 24 hr post transfection. Cells were lysed in homogenate buffer (20 m*M* Tris-HCl [pH 7.4], 0.1% SDS, 0.1% Triton X-100, 0.01% sodium deoxycholate, 1×Complete protease inhibitor cocktail [Roche Diagnostics]). Five micrograms of total protein was separated by 10% PAGE, and the proteins were transferred onto membranes and immunoblotted as described. Blots were probed with a rabbit antibody against LDLR (1:1000; Novus Biologicals, Littleton, CO) and confirmed with a mouse antibody against GAPDH (1:3000; Chemicon).

### *Fluorescence correlation spectroscopy analysis*

To control the total fluorescent signal under saturation, the final concentration of Toc-siRNA-Cy3 or siRNA-Cy3 was fixed at 50 n*M* and varying concentrations of unlabeled Toc-siRNA or unlabeled siRNA respectively (0 to 75 μ*M*) were added to 10-μl aliquots of the HDL fraction. Measurements were performed using the ConfoCor 3 module in combination with a LSM 510 laser scanning microscope (Carl Zeiss

MicroImaging GmbH, Göttingen, Germany) equipped with the C-Apochromat 40×/1.2W objective. A HeNe laser (543 nm) was used for Cy3-labeled siRNA excitation and emission was filtered through a 560- to 615-nm band pass filter. Samples were placed into an eight-well Lab-Tek chambered coverglass (Nalge Nunc International, Rochester, NY) and measured at room temperature. Autocorrelation curves obtained from 10 measurements with a sampling time of 20 sec were fitted with the ConfoCor 3 software package to determine diffusion time of samples.

### *Animals and human cerebrospinal fluid*

Female Crlj:CD1 (ICR) mice aged 3 to 4 months old (27 to 30 g; Oriental Yeast, Tokyo, Japan) were used for ICV infusion experiments. For $LDLR^{-/-}$ mice, B6.129S7-Ldlr (tm1Her)/J (Jackson Laboratory, Bar Harbor, ME) and wild-type (WT) C57BL/6J (Oriental Yeast) were used. Cerebrospinal fluid was collected from a healthy human volunteer. All procedures used in animal studies and the use of human samples were approved by the ethical committee of Tokyo Medical and Dental University and were consistent with local and state regulations as applicable.

### *ICV infusion*

Mice were anesthetized with isoflurane (1.5% to 2.0%). Osmotic minipumps (model 1007D; Alzet, Cupertino, CA) were filled with phosphate-buffered saline (PBS) or free Toc-siBACE or Toc-siBACE/HDL and connected with Brain Infusion Kit 3 (Alzet). A brain-infusion cannula was placed −0.5 mm posterior to the bregma at midline for infusion into the dorsal third ventricle (Thakker *et al.*, 2004).

### *Confocal immunofluorescense and histochemical microscopy analyses*

The fixed brains were sectioned at 10 $\mu$m with a cryostat (Leica, Wetzlar, Germany). For confocal immunofluorescense observation, sections were immunolabeled with antibodies against MAP2 (1:200, AB5622; Chemicon) and glial fibrillary acidic protein (GFAP, 1:500, G3893; Sigma, St. Louis, MO) followed by incubation with fluorescein isothiocyanate (FITC)-conjugated secondary antibodies. Images were obtained with LSM 510 META (Zeiss). Obtained images were transmitted to image analysis software (WinROOF, Mitani, Tokyo, Japan) and analyzed to estimate the areas of each color. To examine regional BACE1 protein expression, sections were immunolabeled with a mouse monoclonal antibody (1:50, MAB5308; Chemicon) in combination with M.O.M. immunodetection kit (Vector Laboratories, Burlingame, CA) and developed with 3,3′-diaminobenzidine (DAB).

### In vivo *analyses for siRNA activity*

Fresh frozen brain samples were sectioned at 10 $\mu$m and transferred onto a membrane slide (Leica), fixed, and dehydrated through a serial gradient of ethanol, 95%, 75%, 50%, 50%, 75%, 95%, 100%, for 30 sec each and once in 100% ethanol for 2 min followed by xylene for 5 min. Sample slides were set on fluorescence equipped laser microdissection system (AS LMD, Leica), and regions of interest were cut at a fixed square measure from three sections (hippocampal formation, $8.4\times10^6$ $\mu m^2$; parietal cortex, $5.1\times10^6$ $\mu m^2$). For qRT-PCR assays, total cellular RNA was extracted (PicoPure RNA isolation kit; Arcturus, Sunnyvale, CA) and total RNA was reverse-transcribed. qRT-PCR was performed as described for the *in vitro* siRNA transfection assay. For Western blots, cut samples were directly collected in 25 $\mu$l of homogenate buffer. Total proteins were separated by 10% PAGE, transferred onto membranes, and immunoblotted as described. For Northern blots, block brain samples, approximately 50 mg each, were homogenized and purified for small RNAs by MirVana (Ambion, Austin, TX). Small RNA samples were loaded 20 $\mu$g for each, separated by 24% denaturing PAGE,

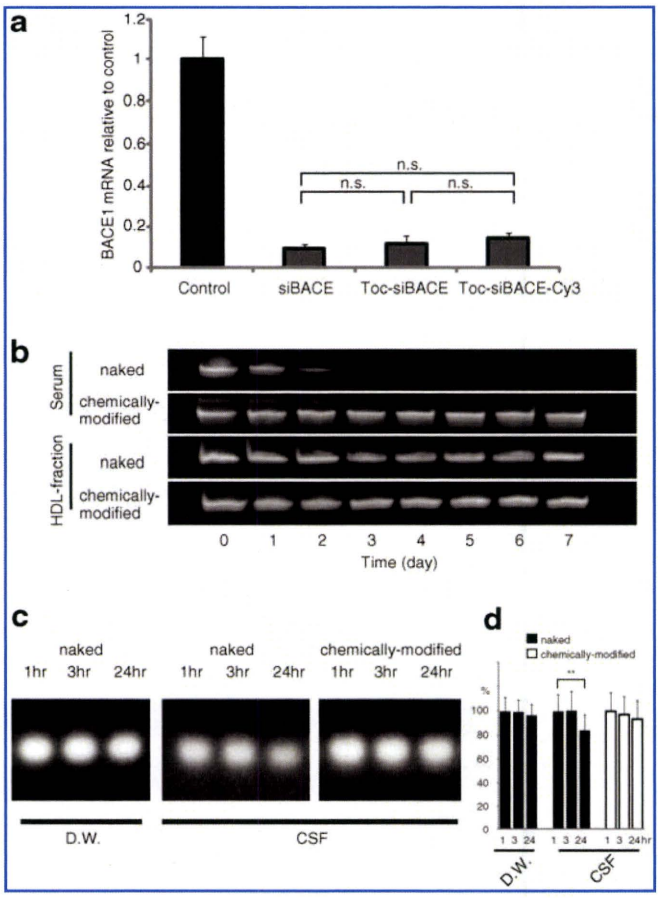


**FIG. 1.** *In vitro* validation of RNAi activity and stability for modified siRNAs against BACE1. **(a)** RNAi activity in mouse Neuro2a cells was measured by transfecting nonconjugated siBACE, Toc-siBACE, and Toc-siBACE-Cy3. Quantitative reverse-transcription polymerase chain reaction (qRT-PCR) analysis of BACE1 mRNA levels showed efficient target silencing after tocopherol conjugation and Cy3 labeling. (Data are shown as mean values ± SEM, $n = 3$. One-way ANOVA followed by Tukey-Kramer multiple comparisons, n.s.; not significant). **(b)** Naked siRNA or chemically modified siRNA was incubated with mouse serum or high-density lipoprotein (HDL) fraction at 37°C for up to 7 days. Samples were separated by nondenaturing 18% PAGE. **(c)** Chemically modified siRNA and naked siRNA were incubated in distilled water (D.W.) or cerebrospinal fluid (CSF) at 37°C up to 24 hr. Samples were separated on nondenaturing 2% agarose. **(d)** Densitometric analysis of the band intensities showed substantial degradation of naked siRNA in CSF. Error bars (SD) are derived from triplicates. $^{**}p < 0.01$, Student's $t$ test.

transferred to nylon membrane (Hybond-N+, Amersham, Piscataway, NJ), and then hybridized with DNA probes labeled by DIG oligonucleotide 3′ end labeling kit (GE Healthcare, Piscataway, NJ). Signals were developed with CDP-Star (GE Healthcare).

## Results

### In vitro *validation of efficiency and stability of Toc-siRNA*

Using Neuro2a cells, we checked RNA interference (RNAi) activity of eight different siRNAs targeting BACE1 mRNA (NM_011792) (siBACE), two from preceding reports (Kao *et al.*, 2004; Singer *et al.*, 2005) and six newly designed sequences, and selected the best siBACE (siBACE-8) (Supplementary Fig. S1a; Supplementary data are available online at www.liebertonline.com/hum). This siBACE was confirmed to suppress endogenous BACE1 protein as well (Supplementary Fig. S1b, c).

α-Tocopherol was covalently bound to the 5′ end of the antisense strand of the siRNA. According to previously reported principles (Nishina *et al.*, 2008), we made chemical modifications with phosphorothioate backbone linkage and sugar 2′-*O*-methylation on both sense and antisense strands for increasing stability of siRNA against endogenous ribonucleases. Furthermore, 5′ end of sense strand was labeled with Cy3 fluorophore to examine histological distribution of Toc-siRNA *in vivo*.

To confirm the influence of α-tocopherol conjugation and Cy3 labeling on RNAi activity, nonconjugated siBACE, Toc-siBACE, and Cy3-labeled Toc-siBACE (Toc-siBACE-Cy3) were transfected to Neuro2a cells at 10 n*M*. These modifications did not influence silencing activity of siBACE (Fig. 1a).

To check the stability of Toc-siBACE against ribonucleases, Toc-siBACE was incubated at 37°C with mouse serum, the HDL fraction of mouse serum, or human CSF. Naked siRNA was completely degraded in serum after incubation for 3 days. Chemically modified siRNA did not degrade for up to 7 days in serum, showing satisfactory protection against ribonucleases. Naked siRNA as well as chemically modified siRNA did not degrade in the HDL fraction after 7 days, suggesting that serum ribonucleases were eliminated after sequential ultracentrifugation (Fig. 1b). With a view to direct central administration, we also checked siRNA stability in CSF. Chemically modified siRNA did not degrade in CSF (Fig. 1c). Naked siRNA showed substantial degradation in CSF after 24 hr by densitometric analysis (Fig. 1d).

### *Toc-siRNA binding assay with HDL*

For simplicity, Toc-siRNA-Cy3 is referred to hereafter as Toc-siRNA. To demonstrate the binding of Toc-siRNA and HDL, we conducted a gel-shift assay for evaluating interaction between these two molecules.

Nonconjugated siRNA incubated with the HDL fraction migrated almost identically to that incubated with PBS. Toc-siRNA incubated with the HDL fraction showed much lower mobility than that with PBS, indicating that the interaction of Toc-siRNA with HDL was due to lipophilic binding by the tocopherol moiety of Toc-siRNA (Fig. 2a). The ratio of

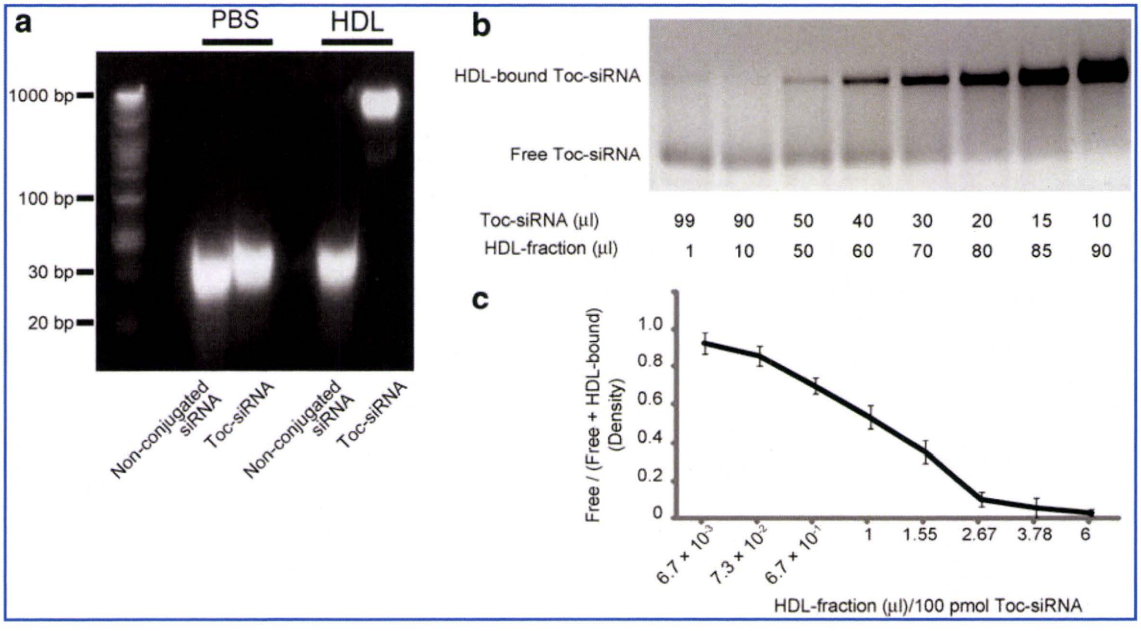


**FIG. 2.** Binding assay for Toc-siRNA and HDL. **(a)** 100 pmol nonconjugated siRNA or Toc-siRNA was added to 10 μl of phosphate-buffered saline (PBS) or the HDL fraction, and then samples were incubated at 37°C for 30 min. When incubated with PBS, Toc-siRNA showed slightly smaller mobility than nonconjugated siRNA on nondenaturing 2% agarose. It was assumed that the size and net charge of the molecule affected the migration change. When incubated with the HDL fraction, Toc-siRNA showed much smaller mobility than that with PBS, indicating the binding between Toc-siRNA and HDL. **(b)** Extensive gel-shift assay for Toc-siRNA and HDL binding. Varying volume ratios of 150 μM Toc-siRNA to HDL fraction were mixed and incubated at 37°C for 10 min. For a gel-shift assay, the loaded amount of Toc-siRNA was equivalent (100 pmol) for each lane and samples were separated on 2% agarose. **(c)** Densitometric analysis of free and HDL-bound Toc-siRNA. The *x*-axis shows the corresponding HDL-fraction volume in **b**. Error bars (SD) are derived from triplicates.

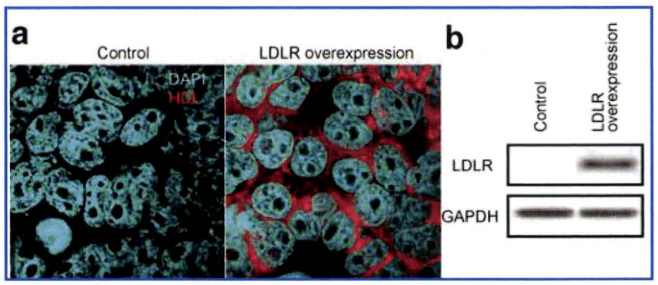


**FIG. 3.** Overexpression of low-density lipoprotein receptor (LDLR) facilitated HDL uptake *in vitro*. Wild-type (WT) and LDLR-overexpressed HEK293T cells were incubated with fluoro-labeled HDL (red signal). **(a)** LDLR-overexpressed cells showed intense signals of labeled HDL with dot-like cytosolic accumulation. **(b)** Western blots of HEK293T cells lysates for LDLR and GAPDH as a loading control.

Toc-siRNA to HDL fraction was determined by an extensive gel-shift assay and optical density measurements with varying ratios of Toc-siRNA to HDL fraction (Fig. 2b and c). The ratio was set at 20 $\mu$l of 150 $\mu M$ Toc-siRNA to 80 $\mu$l of HDL fraction, where free Toc-siRNA almost disappeared. The binding of almost all the Toc-siRNA to HDL was also confirmed by fluorescence correlation spectroscopy analysis (Supplementary Fig. S2).

### *HDL uptake via LDLR* in vitro

We hypothesized that serum HDL can be taken up by neurons and glial cells via LDLR because serum HDL has characteristics similar to HDL-like particles of the central nervous system (CNS) in its size, density, and apolipoproteins. To confirm this, we carried out an LDLR overexpression study *in vitro* by transfecting mouse LDLR-expressing plasmid to HEK293T cells. LDLR expression was confirmed by Western blot analysis (Fig. 3b). The mouse serum HDL fraction was labeled with fluorophore (BODIPY 542/563 C11) and applied to culture medium. LDLR-overexpressed cells showed marked HDL uptake, whereas mock-plasmid–transfected HEK293T cells as a negative control showed almost no HDL uptake (Fig. 3a).

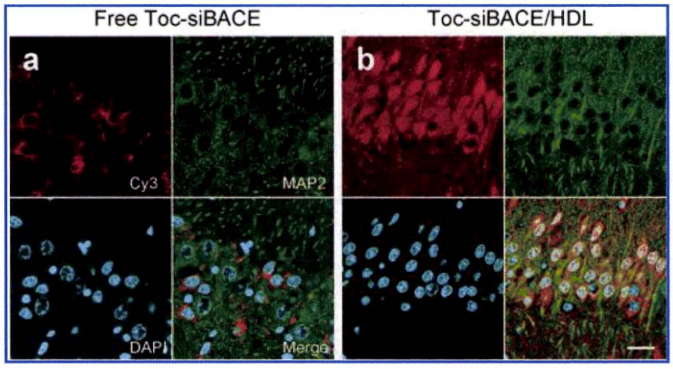


**FIG. 4.** Laser confocal microscopic images of MAP2-labeled hippocampus CA3 neurons infused with either **(a)** free Toc-siBACE or **(b)** Toc-siBACE/HDL. Nuclei were counterstained with 4′,6-diamidino-2-phenylindole (DAPI). Scale bar, 20 $\mu$m.

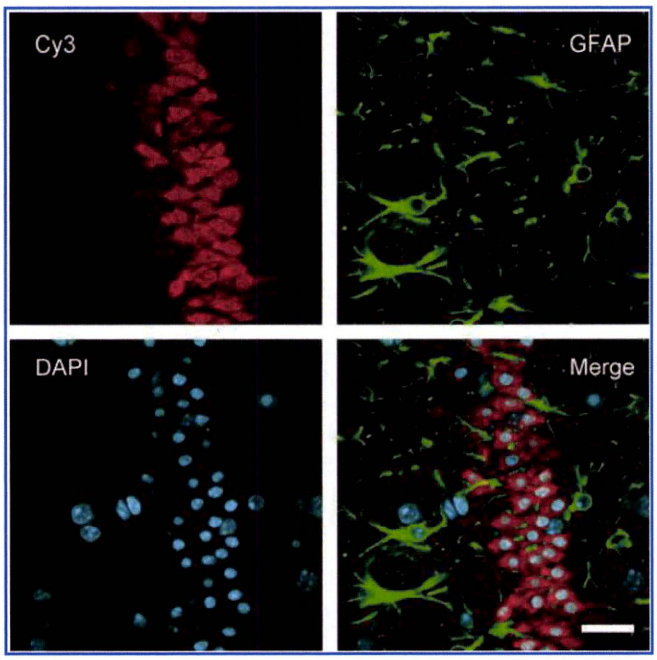


**FIG. 5.** Laser confocal microscopic observation for glial cell uptake of Toc-siBACE in the hippocampus CA3 region of a mouse infused with Toc-siBACE/HDL. Glial cells were detected by anti-GFAP antibody. Nuclei were counterstained with DAPI. Scale bar, 20 $\mu$m.

### *HDL enhanced* in vivo *delivery of Toc-siRNA*

To test the performance of Toc-siRNA/HDL *in vivo*, Toc-siBACE bound to HDL was administered to the mouse brain by direct ICV infusion with osmotic pumps. Continuous ICV infusion of Toc-siBACE/HDL for 7 days achieved broader and more intense transduction of Toc-siBACE to the brain (Fig. 4b) than that of free Toc-siBACE (Fig. 4a), whereas ICV infusion of nonconjugated siBACE showed almost no signal in the brain (Supplementary Fig. S3).

The transduction of Toc-siBACE/HDL distributed broadly within the brain in the posterior frontal, parietal, and temporal areas and the hippocampal formation, and especially in areas more proximal to the lateral and third ventricles. In particular, intense signals were observed in the hippocampal neuronal cell layers and periventricular white matter.

By immunofluorescence microscopic observation, siRNA-transduced cells were mainly neuronal cells detected by anti-MAP2 antibody and showed an intense and homogenous Cy3 signal, rather than tiny dots, in the cytosol and often in the nucleus as well with Toc-siBACE/HDL–infused brain (Fig. 4b). Weaker cytosolic signal was also seen with free Toc-siBACE–infused brain (Fig. 4a). GFAP staining also depicted neuronal rather than glial uptake of Toc-siBACE in the cerebral cortex and hippocampus with Toc-siBACE/HDL–infused brain (Fig. 5).

### In vivo *analyses of RNAi activity in the brain*

To measure the target mRNA reduction in the area where Toc-siRNA was transduced, we used laser dissection microscopy equipped with fluorescent observation system to capture Cy3 signal–positive regions directly. Free Toc-siBACE

could not elicit evident target gene silencing, whereas laser-dissected samples from Toc-siBACE/HDL–infused brain revealed significant reduction of target BACE1 mRNA at the hippocampal formation and parietal cortex (Fig. 6a; free Toc-siBACE vs. Toc-siBACE/HDL, hippocampus; 6% vs. 36%, parietal cortex; 13% vs. 64%, relative to control). Furthermore, neither free nontargeting Toc-siRNA (Toc-siApoB) nor Toc-siApoB/HDL affected target BACE1 mRNA level, indicating sequence specific cleavage.

Moreover, we could detect more prominent band of Dicer-cleaved antisense strand than that of the original antisense strand from Toc-siBACE/HDL–infused brain on siRNA Northern blot (Fig. 6b), indicating efficient delivery of Toc-siBACE to cytosol and its Dicer recognition.

Western blot analysis of BACE1 from signal positive regions in the parietal cortex of Toc-siBACE/HDL–infused brain showed substantial reduction of BACE1 protein (Fig. 6c and d; $\beta$-tubulin as a loading control, 52% reduction to control).

Regional repression of BACE1 protein was also evident by immunohistological examination. We could detect reduced DAB staining in the cerebral cortex, and the hippocampus, where siRNA transduction was confirmed under fluorescence microscopy (Fig. 7). Histological examination by hematoxylin-eosin (HE) staining of the Toc-siBACE/HDL–infused brain showed no obvious abnormality including cellular infiltration (Supplementary Fig. S4).

### *The uptake of Toc-siRNA/HDL was mediated by LDLR*

Glial cells excrete ApoE-containing lipoprotein (HDL-like particles), and neurons incorporate the lipoprotein via receptor-mediated endocytosis. Several members of LDL receptor family (LDLR, low-density lipoprotein receptor-related protein 1 [LRP1], VLDL receptor [VLDLR]) are expressed in neurons and glial cells (Fan *et al.*, 2001). Amongst these receptors, LDLR is a cardinal one for metabolism of HDL-like particles (Vance *et al.*, 2005). We used $LDLR^{-/-}$ mice to see whether Toc-siRNA/HDL uptake is mediated by this receptor. $LDLR^{-/-}$ mice infused with Toc-siBACE/HDL showed much less Cy3 signals in the hippocampal neuronal cell layers than WT mice (Fig. 8a). In the periventricular

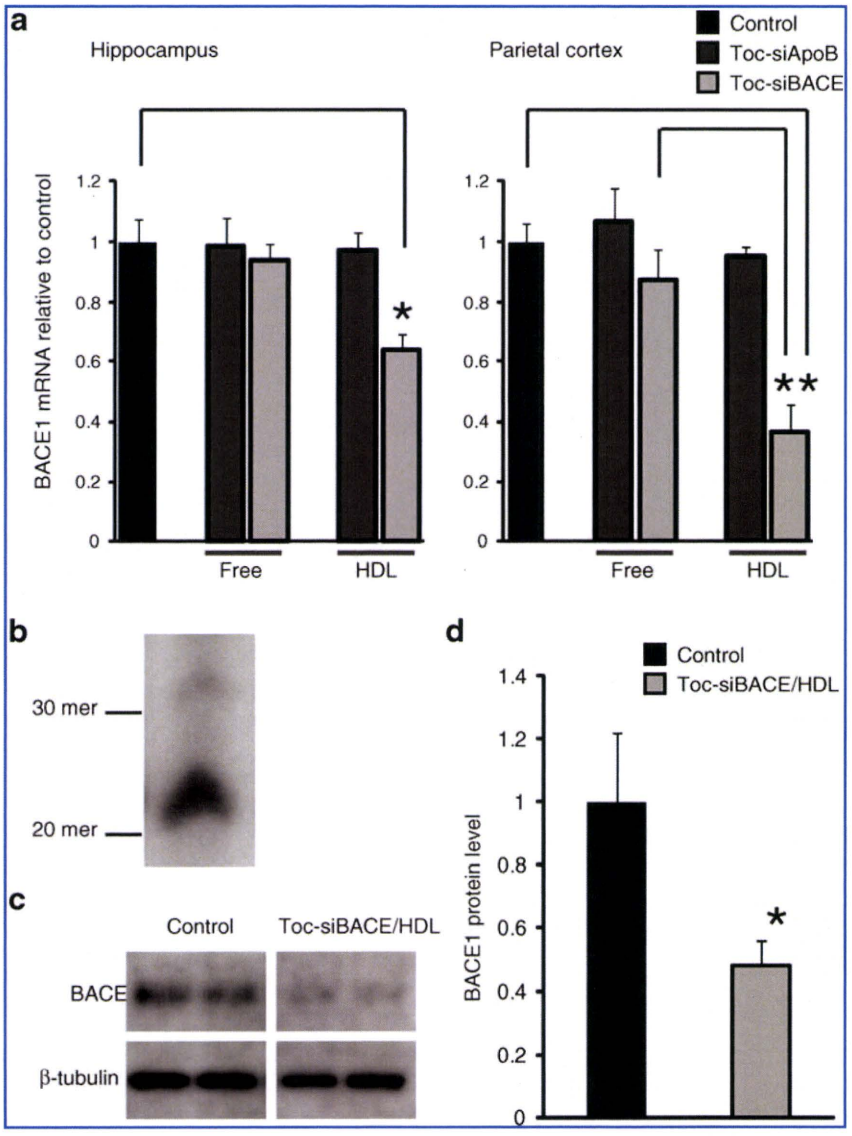


**FIG. 6.** *In vivo* analyses of RNAi activity of free Toc-siBACE and Toc-siBACE/HDL. **(a)** For qRT-PCR analyses, mRNA was purified from laser-dissected samples of the same square measure from each brain region of control brains (PBS infusion), free Toc-siRNA–infused or Toc-siRNA/HDL–infused brains. (Data are shown as mean values ± SEM, $n = 3$. One-way ANOVA followed by Tukey-Kramer multiple comparisons, $^{*}p < 0.05$, $^{**}p < 0.01$). **(b)** Northern blot analysis for Toc-siBACE. Small RNAs were purified from total homogenate of a 3-mm-thick brain section adjacent to the infusion site of the brain. Membrane was proved with the DIG-labeled DNA oligonucleotides of the sense strand. **(c)** For Western blot, total lysates of laser dissected samples of the same square measure from the parietal cortex region were immunoblotted with anti-BACE1 antibody and confirmed with anti-$\beta$-tubulin antibody as a loading control. **(d)** Bar graph shows BACE1/tubulin ratios from densitometry of bands in **c**. Values represent mean ± SEM. $^{*}p = 0.092$, Student's $t$ test.

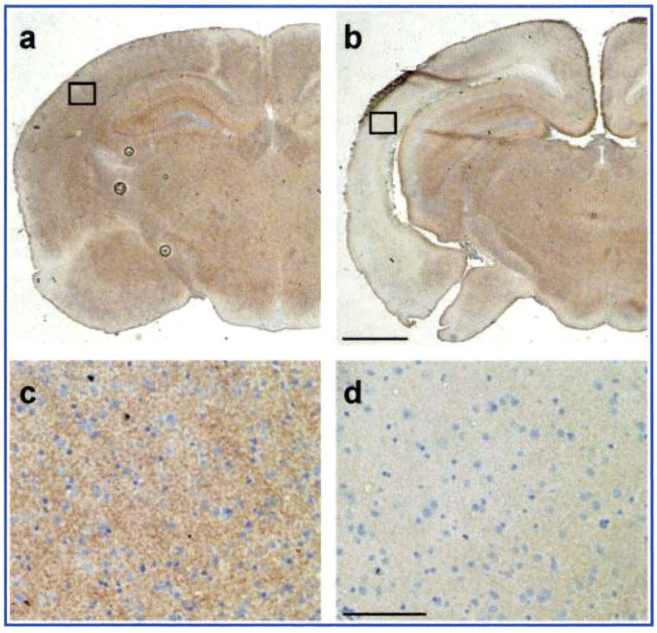


**FIG. 7.** Regional suppression of BACE1 protein by Toc-siBACE/HDL. **(a)** PBS-infused or **(b)** Toc-siBACE/HDL–infused brain sections were immunoperoxidase-stained for BACE1. Reduced DAB staining in the entorhinal, parietal cortex, and hippocampus is shown. Scale bar, 500 $\mu$m. **(c, d)** Panels show insets in **a** and **b**, respectively. Scale bar, 50 $\mu$m.

white matter regions, despite the similar level of Cy3 signals from the extracellular space (red) between WT and LDLR$^{-/-}$ mice, Cy3-positive areas in astrocytes as shown in merged yellow were decreased for LDLR$^{-/-}$ mice compared with WT mice (Fig. 8b). When normalized to the total GFAP-positive green area, the decrease in glial uptake of Toc-siBACE/HDL in LDLR$^{-/-}$ mice was statistically significant (Fig. 8c; WT vs. LDLR$^{-/-}$, $0.306 \pm 0.082$ vs. $0.096 \pm 0.05$, $p = 0.019$).

## Discussion

The ability to direct a particular class of drugs to the brain has been desired for years, but the existence of the blood–brain barrier and the peculiar metabolism of the brain are major obstacles for drug delivery. In this study we developed a new and efficient method of delivering siRNA to the brain by conjugating it with $\alpha$-tocopherol and HDL. Our vector system significantly lowered the dose of siRNA needed for silencing the target mRNA in the CNS.

Similar gene-silencing trials with ICV infusion of non-conjugated siRNA with chemical modifications have been reported (Senn *et al.*, 2005; Senechal *et al.*, 2007). The ICV infusion of free siRNA against dopamine receptor DDAR into the third ventricle of the mouse brain for 7 days could suppress the target mRNA by 60% with phenotypic change (Thakker *et al.*, 2004). Thakker *et al.*, (2004) reported the dose of free siRNA needed was as much as 3 $\mu$mol, whereas we found that just 3 nmol of Toc-siRNA with HDL could induce a target reduction in comparable degree by the same ICV infusion method. The *in vivo* knockdown using antisense oligonucleotides by its ICV infusion was also studied over the last two decades (Godfray and Estibeiro, 2003). Generally, ICV infused antisense oligonucleotides were more readily taken up by brain tissues than free siRNA, but their silencing efficacy is lower than free siRNA (Senn *et al.*, 2005). For example, 4.7 $\mu$mol of an ICV infusion of antisense oligonucleotides to superoxide dismutase 1 was needed to achieve 60% reduction of the target mRNA in the brain (Smith *et al.*, 2006). Roughly speaking, we could get a similar level of silencing effect in the brain with about a 1000-fold lower amount of siRNA with our method compared with ICV infused free siRNA or antisense oligonucleotides. The

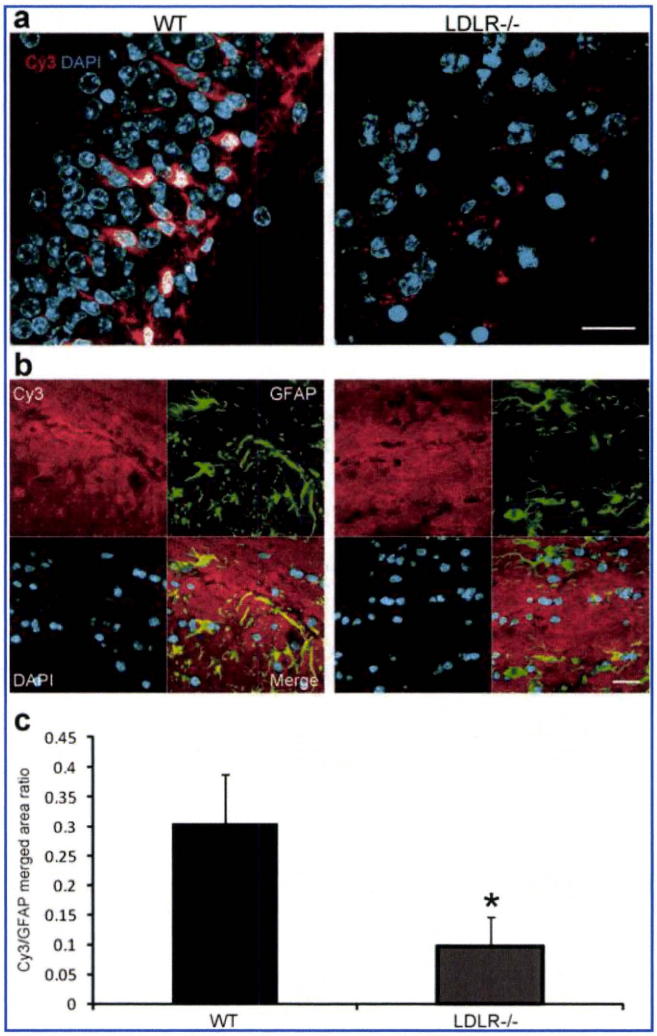


**FIG. 8.** Neuronal and glial uptake of Toc-siRNA/HDL mediated by LDL receptor. WT and LDLR$^{-/-}$ mice were intracerebroventricular (ICV) infused with Toc-siBACE/HDL for 7 days. **(a)** Confocal fluorescence observation revealed reduced uptake of Toc-siBACE/HDL in pyramidal neurons in the hippocampus CA3 of LDLR$^{-/-}$ mice compared with WT. Scale bar, 20 $\mu$m. **(b)** Immunofluorescence confocal observation for glial cells at corpus callosum of WT and LDLR$^{-/-}$ mice. Glial cells were detected by GFAP staining. Scale bar, 20 $\mu$m. **(c)** Bar graph shows Toc-siRNA/HDL uptake area ratio in glial cells from WT and LDLR$^{-/-}$ mice. GFAP and Cy3 positive yellow areas are divided by GFAP-positive green areas. WT, $n = 3$. LDLR$^{-/-}$, $n = 3$. Values represent mean $\pm$ SD. *$p = 0.019$, Student's $t$ test.

direct intraparenchymal brain injection of naked siRNA (Querbes *et al.*, 2009), siRNA with cationic vector (Wang *et al.*, 2005), or cholesterol-conjugated siRNA (DiFiglia *et al.*, 2007) was also studied, but the distribution of siRNA was limited and the procedures were more invasive.

As the cause for our better RNAi effect, we think that our vector system utilizes the physiological lipid metabolism in the brain. The CNS has HDL-like particles that are synthesized mainly by astrocytes to mediate transport of lipids to neurons and glial cells (Vance *et al.*, 2005; Fünfschilling *et al.*, 2007). Since α-tocopherol is a highly lipophilic molecule and astrocytes express αTTP, we assumed that α-tocopherol is transferred from glial cells to neurons via the receptor-mediated pathway with HDL-like particles.

HDL-like particles in the brain contain ApoE as a major apolipoprotein, which is to be the ligand for the receptor-mediated endocytosis by LDLR and LRP1 in neurons (Rothe and Müller, 1991; Posse *et al.*, 2000). In addition, astrocytes also express LDLR and LRP-1 (LaDu, 2000; Rapp *et al.*, 2006) and internalize HDL-like particles. HDL-like particles and serum HDL are similar to each other in density and size, and both have ApoE and ApoA-1 (Pitas *et al.*, 1987). Since it was shown that rat sympathetic neurons can take up serum LDL and HDL as well as HDL-like particles via its LDLR (Rothe and Müller, 1991), we used serum HDL as a vector to deliver Toc-siRNA to neurons. Significant knockdown of endogenous BACE1 mRNA by ICV infusion of Toc-siRNA/HDL could not be obtained without binding to HDL, and moreover the delivery was much lower in $LDLR^{-/-}$ mouse brains. With these results, we believe that this vector system utilizes the physiological receptor-mediated lipid metabolism pathway of the brain, but not simple diffusion or macropinocytosis, to deliver siRNA. However, the uptake of Toc-siRNA/HDL in $LDLR^{-/-}$ mice was not completely diminished, suggesting that other lipoprotein receptors such as LRP1 or megalin, or another uptake mechanism of siRNA, such as a SID-1–mediated pathway in hepatocytes (Duxbury *et al.*, 2005), might contribute to the remaining uptake.

Although the delivery efficiency of siRNA by our vector system is better than previously reported, the reduction of the target mRNA of BACE1 was as much as 60% to 70%. Even partial reduction of BACE1, however, is suggested to have a dramatic effect on Alzheimer pathology in AD model mice with mutant amyloid precursor protein (APP). Single allele ablation caused only a 12% decrease in Aβ level, but nonetheless resulted in four- to fivefold fewer Aβ plaques (McConlogue *et al.*, 2007). Similarly, only 40% reduction of BACE1 protein by directly injected siRNA-expressing lentivirus significantly reduced AD pathology (Singer *et al.*, 2005). Additionally, duplication of the *APP* gene with a 1.5-fold gene dosage increase is known to cause familial AD (Blom *et al.*, 2008), suggesting that a 33% reduction of APP expression is enough to prevent the disease. Therefore, a more than 60% reduction of BACE1 with our vector system can be expected to reduce Aβ load and improve AD phenotype.

Together, we could achieve highly efficient gene silencing in the brain by ICV infusion of Toc-siRNA/HDL that should utilize the receptor-mediated physiological pathway. That resulted in lower doses by orders of magnitude than needed in previously reported methods for nucleotide delivery to the brain.

**Acknowledgments**

This work was supported by grants from the Japanese Society for the Promotion of Science (#20023010) and the Japan Foundation for Neuroscience and Mental Health (#2212070).

**Author Disclosure Statement**

The authors declare no competing financial interests.

**References**

Akinc, A., Goldberg, M., Qin, J., *et al.* (2009). Development of lipidoid-siRNA formulations for systemic delivery to the liver. Mol. Ther. 17, 872–879.

Akinc, A., Zumbuehl, A., Goldberg, M., *et al.* (2008). A combinatorial library of lipid-like materials for delivery of RNAi therapeutics. Nat. Biotechnol. 5, 561–569.

Blom, E.S., Viswanathan, J., Kilander, L., *et al.* (2008). Low prevalence of APP duplications in Swedish and Finnish patients with early-onset Alzheimer's disease. Eur. J. Hum. Genet. 2, 171–175.

DiFiglia, M., Sena-Esteves, M., Chase, K., *et al.* (2007). Therapeutic silencing of mutant huntingtin with siRNA attenuates striatal and cortical neuropathology and behavioral deficits. Proc. Natl. Acad. Sci. U. S. A. 43, 17204–17209.

Duxbury, M.S., Ashley, S.W., and Whang, E.E. (2005). RNA interference: a mammalian SID-1 homologue enhances siRNA uptake and gene silencing efficacy in human cells. Biochem. Biophys. Res. Commun. 2, 459–463.

Fan, Q., Iosbe, I., Asou, H., *et al.* (2001). Expression and regulation of apolipoprotein E receptors in the cells of the central nervous system in culture: A review. J. Am. Aging. Assoc. 24, 1–10.

Fünfschilling, U., Saher, G., Xiao, L., *et al.* (2007). Survival of adult neurons lacking cholesterol synthesis in vivo. BMC Neurosci. 8, 1.

Gao, S., Dagnaes-Hansen, F., Nielsen, E.J., *et al.* (2009). The effect of chemical modification and nanoparticle formulation on stability and biodistribution of siRNA in mice. Mol. Ther. 7, 1225–1233.

Godfray, J., and Estibeiro, P. (2003). The potential of antisense as a CNS therapeutic. Expert Opin. Ther. Targets. 3, 363–376.

Gohil, K., Oommen, S., Quach, H.T., *et al.* (2008). Mice lacking alpha-tocopherol transfer protein gene have severe alpha-tocopherol deficiency in multiple regions of the central nervous system. Brain Res. 1201, 167–176.

Goti, D., Balazs, Z., Panzenboeck, U., *et al.* (2002). Effects of lipoprotein lipase on uptake and transcytosis of low density lipoprotein (LDL) and LDL-associated alpha-tocopherol in a porcine in vitro blood-brain barrier model. J. Biol. Chem. 32, 28537–28544.

Hatch, F.T., and Lees, R.S. (1968). Practical methods for plasma lipoprotein analysis. Advan. Lipid Res. 6, 1–68.

Herz, J., and Chen, Y. (2006). Reelin, lipoprotein receptors and synaptic plasticity. Nat. Rev. Neurosci. 11, 850–859.

Hosomi, A., Goto, K., Kondo, H., *et al.* (1998). Localization of alpha-tocopherol transfer protein in rat brain. Neurosci. Lett. 3, 159–162.

Kao, S.C., Krichevsky, A.M., Kosik, K.S., and Tsai, L.H. (2004). BACE1 suppression by RNA interference in primary cortical neurons. J. Biol. Chem. 3, 1942–1949.

Kappus, H., and Diplock, A.T. (1992). Tolerance and safety of vitamin E: a toxicological position report. Free Radic. Biol. Med. 1, 55–74.

Kim, D.H., Behlke, M.A., Rose, S.D., *et al.* (2005). Synthetic dsRNA Dicer substrates enhance RNAi potency and efficacy. Nat. Biotechnol. 2, 222–226.

Kumar, P., Wu, H., McBride, J.L., *et al.* (2007). Transvascular delivery of small interfering RNA to the central nervous system. Nature 7149, 39–43.

LaDu, M.J. (2000). Apolipoprotein E receptors mediate the effects of beta-amyloid on astrocyte cultures. J. Biol. Chem. 43, 33974–33980.

Lima, W.F., Murray, H., Nichols, J.G., *et al.* (2009). Human Dicer binds short single-strand and double-strand RNA with high affinity and interacts with different regions of the nucleic acids. J. Biol. Chem. 4, 2535–2548.

Mardones, P., Strobel, P., Miranda, S., *et al.* (2002). Alpha-tocopherol metabolism is abnormal in scavenger receptor class B type I (SR-BI)-deficient mice. J. Nutr. 3, 443–449.

McConlogue, L., Buttini, M., Anderson, J.P., *et al.* (2007). Partial reduction of BACE1 has dramatic effects on Alzheimer plaque and synaptic pathology in APP Transgenic Mice. J. Biol. Chem. 282, 26326–26334.

Moschos, S.A., Williams, A.E., and Lindsay, M.A. (2007). Cell-penetrating-peptide-mediated siRNA lung delivery. Biochem. Soc. Trans. 4, 807–810.

Nishina, K., Unno, T., Uno, Y., *et al.* (2008). Efficient in vivo delivery of siRNA to the liver by conjugation of alpha-tocopherol. Mol. Ther. 4, 734–740.

Pfrieger, F.W. (2003). Cholesterol homeostasis and function in neurons of the central nervous system. Cell Mol. Life Sci. 6, 1158–1171.

Pitas, R.E., Boyles, J.K., Lee, S.H., *et al.* (1987). Lipoproteins and their receptors in the central nervous system. J. Biol. Chem. 29, 14352–14360.

Posse De Chaves, E.I., Vance, D.E., Campenot, R.B., *et al.* (2000). Uptake of lipoproteins for axonal growth of sympathetic neurons. J. Biol. Chem. 26, 19883–19890.

Qian, J., Morley, S., Wilson, K., *et al.* (2005). Intracellular trafficking of vitamin E in hepatocytes: the role of tocopherol transfer protein. J. Lipid Res. 10, 2072–2082.

Querbes, W., Ge, P., Zhang, W., *et al.* (2009). Direct CNS Delivery of siRNA Mediates Robust Silencing in Oligodendrocytes. Oligonucleotides 1, 23–30.

Rapp, A., Gmeiner, B., and Hüttinger, M. (2006). Implication of apoE isoforms in cholesterol metabolism by primary rat hippocampal neurons and astrocytes. Biochimie 5, 473–483.

Rigotti, A. (2007). Absorption, transport, and tissue delivery of vitamin E. Mol. Aspects Med. 5–6, 423–436.

Rothe, T., and Müller, H.W. (1991). Uptake of endoneurial lipoprotein into Schwann cells and sensory neurons is mediated by low density lipoprotein receptors and stimulated after axonal injury. Neurochem. 6, 2016–2025.

Rozema, D.B., Lewis, D.L., Wakefield, D.H., *et al.* (2007). Dynamic PolyConjugates for targeted in vivo delivery of siRNA to hepatocytes. Proc. Natl. Acad. Sci. USA. 32, 12982–12987.

Senechal, Y., Kelly, P.H., Cryan, J.F., *et al.* (2007). Amyloid precursor protein knockdown by siRNA impairs spontaneous alternation in adult mice. J. Neurochem. 6, 1928–1940.

Senn, C., Hangartner, C., Moes, S., *et al.* (2005). Central administration of small interfering RNAs in rats: a comparison with antisense oligonucleotides. Eur. J. Pharmacol. 1–3, 30–37.

Singer, O., Marr, R.A., Rockenstein, E., *et al.* (2005). Targeting BACE1 with siRNAs ameliorates Alzheimer disease neuropathology in a transgenic model. Nat. Neurosci. 10, 1343–1349.

Smith, R.A., Miller, T.M., Yamanaka, K., *et al.* (2006). Antisense oligonucleotide therapy for neurodegenerative disease. J. Clin. Invest. 8, 2290–2296.

Thakker, D.R., Natt, F., Hüsken, D., *et al.* (2004). Neurochemical and behavioral consequences of widespread gene knockdown in the adult mouse brain by using nonviral RNA interference. Proc. Natl. Acad. Sci. USA. 49, 17270–17275.

Vance, J.E., Hayashi, H., and Karten, B. (2005). Cholesterol homeostasis in neurons and glial cells. Semin. Cell Dev. Biol. 2, 193–212.

Wang, Y.L., Liu, W., Wada, E., *et al.* (2005). Clinico-pathological rescue of a model mouse of Huntington's disease by siRNA. Neurosci. Res. 3, 241–249.

Wolfrum, C., Shi, S., Jayaprakash, K.N., *et al.* (2007). Mechanisms and optimization of in vivo delivery of lipophilic siRNAs. Nat. Biotechnol. 10, 1149–1157.

Yokota, T., Igarashi, K., Uchihara, T., *et al.* (2001). Delayed-onset ataxia in mice lacking alpha-tocopherol transfer protein: model for neuronal degeneration caused by chronic oxidative stress. Proc. Natl. Acad. Sci. USA. 26, 15185–15190.

Yu, L., Tan, M., Ho, B., *et al.* (2006). Determination of critical micelle concentrations and aggregation numbers by fluorescence correlation spectroscopy: aggregation of a lipopolysaccharide. Anal. Chim. Acta 1, 216–225.

Zimmermann, T.S., Lee, A.C., Akinc, A., *et al.* (2006). RNAi-mediated gene silencing in non-human primates. Nature 441, 111–114.

Address correspondence to:
*Takanori Yokota*
*Department of Neurology and Neurological Science*
*Tokyo Medical and Dental University*
*1-5-45 Yushima*
*Bunkyo-ku*
*Tokyo 113-8519*
*Japan*

*E-mail:* tak-yokota.nuro@tmd.ac.jp

Received for publication November 7, 2010;
accepted after revision December 17, 2010.

Published online: December 17, 2010.

Biochemical and Biophysical Research Communications 405 (2011) 204–209

Contents lists available at ScienceDirect

Biochemical and Biophysical Research Communications

journal homepage: www.elsevier.com/locate/ybbrc

# Intraperitoneal AAV9-shRNA inhibits target expression in neonatal skeletal and cardiac muscles

Azat Mayra [a], Hiroyuki Tomimitsu [a], Takayuki Kubodera [a], Masaki Kobayashi [a], Wenying Piao [a], Fumiko Sunaga [a], Yukihiko Hirai [b], Takashi Shimada [b], Hidehiro Mizusawa [a], Takanori Yokota [a,*]

[a] Department of Neurology and Neurological Science, Graduate School, Tokyo Medical and Dental University, 1-5-45 Yushima, Bunkyo-ku, Tokyo 113-8519, Japan
[b] Department of Biochemistry and Molecular Biology, Nippon Medical School, 1-1-5 Sendagi, Bunkyo-ku, Tokyo 113-8602, Japan

ARTICLE INFO

*Article history:*
Received 24 November 2010
Available online 8 January 2011

*Keywords:*
shRNA
AAV9
Neonatal

ABSTRACT

Systemic injections of AAV vectors generally transduce to the liver more effectively than to cardiac and skeletal muscles. The short hairpin RNA (shRNA)-expressing AAV9 (shRNA-AAV9) can also reduce target gene expression in the liver, but not enough in cardiac or skeletal muscles. Higher doses of shRNA-AAV9 required for inhibiting target genes in cardiac and skeletal muscles often results in shRNA-related toxicity including microRNA oversaturation that can induce fetal liver failure.

In this study, we injected high-dose shRNA-AAV9 to neonates and efficiently silenced genes in cardiac and skeletal muscles without inducing liver toxicity. This is because AAV is most likely diluted or degraded in the liver than in cardiac or skeletal muscle during cell division after birth. We report that this systemically injected shRNA-AAV method does not induce any major side effects, such as liver dysfunction, and the dose of shRNA-AAV is sufficient for gene silencing in skeletal and cardiac muscle tissues. This novel method may be useful for generating gene knockdown in skeletal and cardiac mouse tissues, thus providing mouse models useful for analyzing diseases caused by loss-of-function of target genes.



## 1. Introduction

Since the discovery that RNA interference (RNAi), mediated by small interference RNA (siRNA), can inhibit target gene expression, RNAi has become the standard tool for sequence-specific knockdown of gene expression in molecular biology [1]. RNAi biology utilizes short hairpin RNA (shRNA) usually expressed from plasmid or viral vectors. Base-pair stems and a loop region characterize shRNAs. Different types of promoters can be used for shRNA expression and, therefore, various knockdown models using tissue- or cell-specific promoters for target genes can be generated [2].

Another small RNA, microRNA (miRNA), is known to bind endogenous non-protein coding genes, with the precursors of miRNAs being hairpin structures similar to shRNAs. The miRNA and shRNA are known to utilize the common pathways of exportin-5 for nuclear export and the processing by Dicer and Argonaute family proteins in the cytoplasm. As these processes are competed for by miRNA and shRNA, a high level of shRNA expression could interfere with miRNA maturation and cause damage to the cells [1,4]. From these view points, properly designed and expressed shRNAs are necessary to establish knockdown models of chronic diseases that are both acquired and inherited.

For generating in vivo models of disease by using shRNAs, the main constraint is the difficulty in delivering the shRNA to the target tissues. Delivery of gene vectors to local skeletal muscles and cardiac muscle has been achieved by direct intramuscular injection or by local blood perfusion with nonviral and viral vectors, including plasmid DNA and adeno-associated virus (AAV) [5,6]. A number of AAV serotype vectors are available, with AAV1, 6, 8 and 9 being reported to efficiently express the transgenes in skeletal and cardiac muscles [7–11]. However, there are only a few reports claiming that systemic AAV-shRNA vector injection can significantly inhibit target genes in skeletal muscle. One paper showed a significant reduction of the target gene in skeletal muscle and liver by using tail vein injection of AAV type 6 [12], yet liver function was not examined. In our preliminary study, intravenously administered high dose AAV8- or AAV9-shRNA ($1 \times 10^{12}$ v.g./mouse) achieved substantial inhibition of the target gene in the liver, but induced severe liver damage without sufficient gene silencing in the skeletal muscle itself. Intraperitoneal administration of AAV vectors in neonatal mice showed significantly higher expression of target genes than in adult mice. Moreover, using systemic administration of AAV vectors in neonatal mice, target genes can be delivered to neurons and cardiac and skeletal muscle more efficiently [10,13–16]. In this study, we injected AAV9-shRNA intraperitoneally to neonates and sufficiently inhibited the target genes in skeletal and cardiac muscles without detecting any side effects, including liver damage.

* Corresponding author. Fax: +81 3 5803 0169.
*E-mail address:* tak-yokota.nuro@tmd.ac.jp (T. Yokota).

0006-291X/$ - see front matter © 2011 Elsevier Inc. All rights reserved.
doi:10.1016/j.bbrc.2011.01.009

## 2. Materials and methods

### 2.1. Construction of the anti-SOD1 shRNA AAV9 vector

We prepared the anti-SOD1 shRNA cassette as previously reported [17]. The anti-SOD1 shRNA cassette was cloned downstream of the polymerase III (PolIII) human U6 promoter in the AAV vector (Stratagene, La Jolla, CA, USA) plasmid (Fig. 1). The silencing efficiency of the anti-SOD1 shRNA sequence was verified using several cultured cell lines and transgenic mice expressing the anti-SOD1 shRNA, as previously described [3]. Human growth hormone polyadenylation (hGH poly A) cassette (Stratagene) was inserted downstream of the shRNA sequence in the vector for the titration assay of the vector by quantitative real-time PCR (Fig. 1).

### 2.2. Production and titration of the anti-SOD-shRNA AAV9 vector

The recombinant viral vector was produced according to the three-plasmid transfection protocol using the calcium phosphate method [18]. Human embryonic kidney cultured cells (HEK 293 cells) at approximately 70% confluence were transfected with the AAV9 packaging plasmid, pRep2/Cap9 (a kind gift from Wilson J), adenovirus Helper plasmid (Stratagene), and the pAAV-anti-SOD1-shRNA plasmid, at a ratio of 1:1:1. At 6 h post-transfection the medium was replaced with fresh culture medium containing 2% fetal bovine serum (Sigma, St. Louis, MO, USA), and the cells were cultured for 48 h at 37 °C. After the incubation, the cells were harvested and pelleted by centrifugation at 4000 rpm. The pellets were then resuspended in Tris–HCl (pH 8.5), and after treatment with 5% sodium deoxycholate for 30 min at 37 °C, the cells were subjected to three freeze–thaw cycles. The cell suspension was treated with Benzonase (Merck, Darmstadt, Denmark), followed by the process of ammonium sulfate deposition using $(NH_4)_2SO_4$ (pH 8.5). Cell pellets contained the AAV dissolved in phosphate buffered saline (PBS), and the viral solution was layered with Optiprep (Axis-shield, Oslo, Norway). After centrifugation of the solution at 52,000 rpm for 17 h at 15 °C, the viral fractions were collected from the bottom of the gradient.

Genome titers of the AAV vectors were determined by quantitative PCR using the TaqMan system. The following primers and probes targeting the polyA signal were used: 5′-CAGGCTGGTC TCCAACTCCTC-3′ and 5′-GCAGTGGTTCACGCCTGTAA-3′ served as the primer set, and 5′-TACCCACCTTGGCCTC-3′ served as the probe.

### 2.3. Animals

All of the animal procedures were performed in accordance with the protocols approved by the Animal Experiment Committee of Tokyo Medical and Dental University (#0100101). All of the ICR mice were obtained from Orient Yeast Co. Ltd. (Tokyo, Japan). Postnatal day-1 ICR mice were injected intraperitoneally with $5 \times 10^{11}$ vector genome per gram (v.g./g) of the anti-SOD1 shRNA AAV9 vector ($n = 4$). Non-injected littermates were used as the control group ($n = 4$). The body weights of the mice were measured chronologically. At 4 weeks after the injection, all of the mice were euthanized after performing the rotarod tests. Blood, skeletal muscles (quadriceps and hamstrings), cardiac muscle, and liver tissues were collected for analysis.

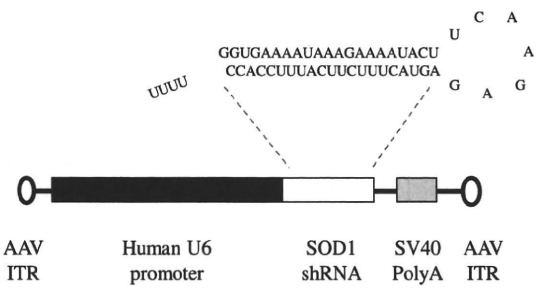


**Fig. 1.** Construction of the anti-SOD1 shRNA AAV9 vector. The anti-SOD1 shRNA expression AAV9 vector including an anti-SOD1 shRNA between the polymerase III human U6 promoter and hGH polyA cassette.

### 2.4. Rotarod test

The rotarod test was performed using the accelerating Rotarod (Ugo Basile Biological Research Apparatus, Varese, Italy). The 4-week-old mice in both groups were placed on the rod (3 cm diameter) in four trials each day, for a series of 4 days. Each trial lasted up to a maximum of 10 min; the time spent on the rod without falling was recorded. The average time of each group was calculated and statistical significance was assessed by one-way ANOVA. Significance was defined as $p < 0.05$.

### 2.5. Northern blotting analysis of shRNA

The RNAs were derived from quadriceps, hamstrings, cardiac muscle, and liver using MirVana (Ambion, Austin, TX, USA). Three micrograms of RNA derived from each tissue were separated on 18% polyacrylamide-urea gels, and transferred to Hybond-N+ membranes (GE Healthcare, Piscataway, UK). The blots were hybridized with a probe against the antisense sequence of the shRNA. The probe sequence was 5′-GGTGGAAATGAAGAAAGTAC-3′. The probe was labeled using DIG Oligonucleotide 3′-End Labeling Kit 2nd Generation (Roche, Penzberg, Germany). The signal was visualized using the Gene Images CDP-star detection kit (GE Healthcare).

### 2.6. Measurement of RNA reduction by quantitative RT-PCR

Total RNAs were extracted from the collected tissues using Isogen (Nippon Gene, Toyama, Japan). DNase-treated total RNAs (0.5 μg) were reverse transcribed using SuperScript III Reverse Transcriptase (Invitrogen, Carlsbad, CA, USA). The cDNAs were amplified by the quantitative TaqMan system on a Light Cycle 480 Real-Time PCR Instrument (Roche), according to the manufacturer's protocol. SOD1 mRNA expression level in each tissue was measured using the primers and probe designed as follows: Forward primer: 5′-GGTGCAGGGAACCATCCA-3′, reverse primer: 5′-CCCATGCTGGCCTTCAGT-3′, and the probe: 5′-AGGCAAGCGGTGAA CCAGTTGTGTTG-3′. In order to normalize the RT-PCR values, the cDNAs were also amplified quantitatively with the TaqMan primers and the probe sets for GAPDH (Applied Biosystems, Warrington, UK). The ratio of SOD1 mRNA expression level to GAPDH expression was calculated to estimate the shRNA silencing efficiency. Significant differences between the two groups were calculated with the Welch's *T*-test.

### 2.7. Western blotting

Protein samples were extracted from the liver, hamstrings and cardiac muscles. The tissues were homogenized in cold homogenization buffer containing 0.1% sodium dodecylsulfate (SDS), 1% sodium deoxycholate, 1% Triton X-100, and 1 mM phenylmethylsulfonyl fluoride, together with a protein inhibitor cocktail (Roche). Eight micrograms of the extracted protein of each sample was mixed with laemmli sample buffer (BioRad, Hercules, CA, USA), denatured at 95 °C for 5 min, and separated on a 15% SDS–PAGE gel. The separated proteins were transferred to a polyvinylidene difluoride membrane (BioRad), and incubated with the specific primary antibodies, rabbit anti-SOD1 antibody (StressGen Biotechnologies, Victoria, British Columbia, Canada) and mouse anti-GAPDH

monoclonal antibody (Biodesign, Saco, ME, USA). After incubation, the membrane was rinsed and incubated with 0.1% horseradish peroxidase conjugated secondary antibodies, goat anti-rabbit HRP IgG and goat anti-mouse HRP IgG (Thermo Science, Rockford, IL, USA). Protein–antibody interactions were visualized using the supersignal west femto maximum sensitivity substrate (Thermo Science).

### 2.8. Pathological examinations

The skeletal muscles were frozen rapidly in liquid-nitrogen-cooled isopentane, and the liver and cardiac muscles were fixed in 10% formalin and embedded in paraffin. Ten-microgram frozen sections of skeletal muscles and 5-μm paraffin sections of liver and cardiac muscle were processed for hematoxylin and eosin staining.

### 2.9. Blood chemistry examinations

The sera were prepared from blood samples of the mice. In order to evaluate liver and muscle function, serum alanine aminotransferase (ALT), aspartate aminotransferase (AST), alkaline phosphatase (ALP), lactate dehydrogenase (LDH), total bilirubin (T-BIL), albumin (ALB), total protein (TP), and creatine kinase (CK) were measured (Oriental Yeast Co. Ltd., Tokyo, Japan). Statistically significant differences between the injected group and the control group were calculated by the Welch's *T*-test.

## 3. Results

### 3.1. Growth and health status of the injected mice

After the mice were injected with anti-SOD1 shRNA AAV9, they were raised together with their littermate controls for 4 weeks. The body weights of the injected mice and their littermate controls were similar (Fig. 2A). In the accelerating rotarod tests, there were no significant differences in motor function between the injected mice and littermate controls (Fig. 2B). At the end of the experimental period, the mice were dissected and showed no morphological abnormalities such as hepatomegaly, cardiomegaly, ascites, pleural effusion, edema, body fluid retention, or adhesion of organs.

### 3.2. Tissue expression of anti-SOD1 shRNA

Expression of anti-SOD1 shRNA in the liver, quadriceps, hamstrings and cardiac muscles was demonstrated by northern blot analysis (Fig. 3A). Fifty-four nucleotides (nt) of shRNA were not detected in these tissues (data not shown); however, a 21-nt antisense strand of siRNA was detected. This finding clearly indicates that the expressed anti-SOD1 shRNA was almost completely processed by Dicer. The expression level of the antisense siRNA was robust in cardiac and hamstring muscles, but surprisingly, much less in quadriceps muscles. Importantly, expression of siRNA was not detected in the liver.

### 3.3. The inhibitory effect of SOD1 mRNA

Quantitative RT-PCR showed that the expression level of SOD1 mRNA in the cardiac and hamstrings muscles of the injected mice was significantly reduced in comparison with those of the littermate controls. Using this method of injection, we observed approximately 80% reduction of SOD1 mRNA in the cardiac muscles and 65% reduction in the hamstrings. However, reduction of SOD1 mRNA in the quadricep muscles and liver were mild or absent (Fig. 3B). Effective suppression of the SOD1 gene was also confirmed at the protein level by Western blot analysis. Expression of the SOD1 protein was markedly reduced in the cardiac and hamstring muscles, but reduction in the liver was not clear (Fig. 3C).

### 3.4. Pathological examinations

HE staining of the injected mouse specimens showed no inflammatory changes in cardiac and skeletal muscles or in the liver (Fig. 4). In the hamstring muscle, we found no abnormal fibers such as small angular fibers, necrotic or regenerative muscle fibers. In the cardiac muscle, abnormal findings such as interstitial proliferation and muscle fiber degeneration were not seen. In the liver pathology, we found no structural abnormalities such as hepatic lobules.

### 3.5. Blood chemistry examinations

Serum AST, ALT, ALP, LDH, CK, ALB and TP values in both groups are shown in Table 1. Serum AST, ALT and LDH were increased

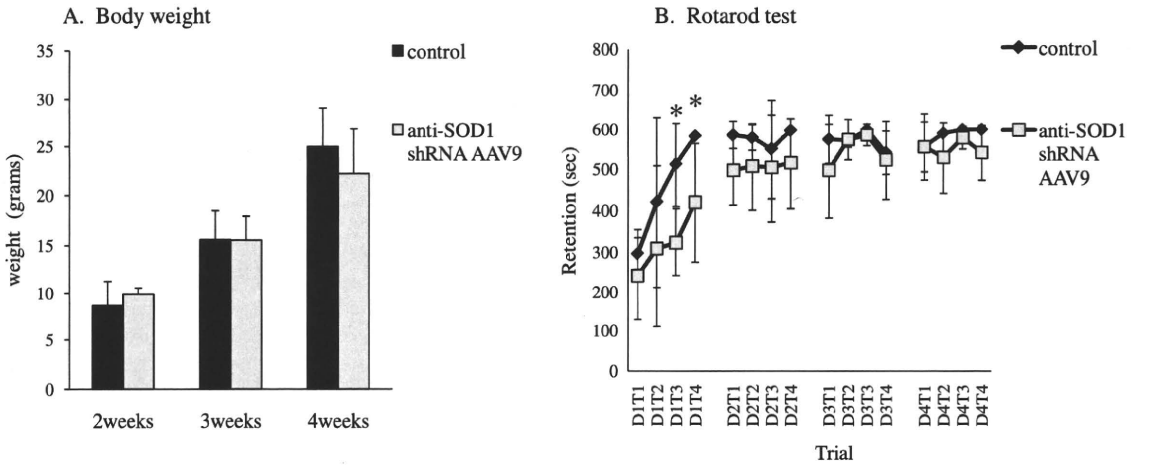


**Fig. 2.** Mouse growth and movement ability. (A) During the 4-week experimental period, none of the anti-SOD1 shRNA AAV9 vector-injected mice showed any significant differences in body weight compared with the littermate controls. Data are presented as the mean with SD ($n = 4$ for each group, $p > 0.05$). (B) In the accelerating rotarod test 4 weeks after injection of the anti-SOD1 shRNA AAV9 vector, all of the mice could perform the task similar to that of the littermate controls. Each mouse was trained in four trials each day (T1–T4), for a series of 4 days (D1–D4). Except for the third and fourth test of the first day (in the D1T3 $p = 0.025$, in the D1T4 $p = 0.048$), there was no significant difference between the injected mouse group and the littermate control group. Data are presented as the mean with SD ($n = 4$ for each group, $p > 0.05$).

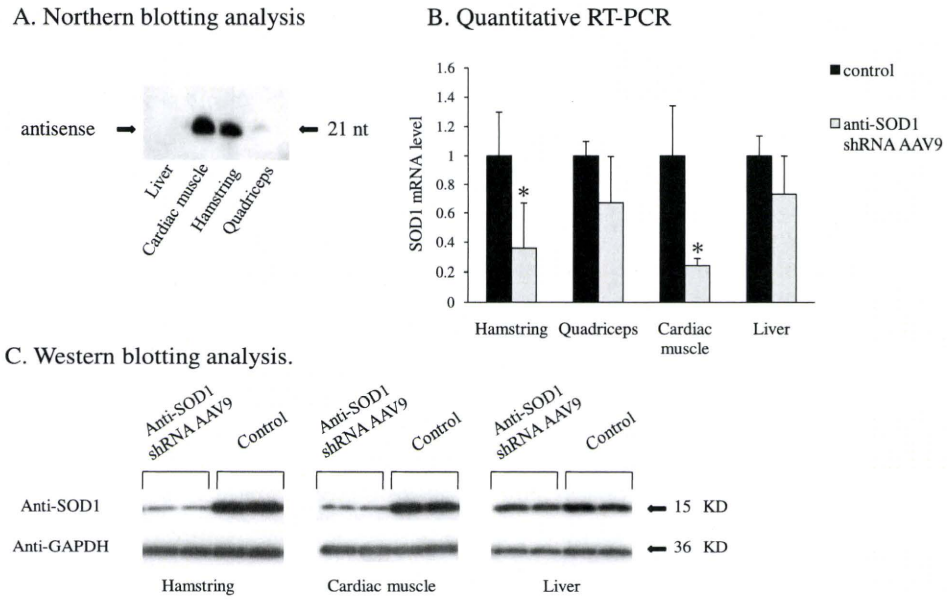


**Fig. 3.** Expression of shRNA and reduction efficiency of the anti-SOD1 shRNA AAV9 vector. (A) Northern blotting analysis of the total RNA derived from the liver, quadriceps, hamstrings, and cardiac muscles at 4 weeks after injection. The 21 nt antisense bands processed from shRNA are detected. Anti-SOD1shRNA is expressed higher in cardiac and hamstring muscles but shows lower expression in quadricep muscle and liver. (B) Quantitative RT-PCR of SOD1 mRNA in the liver, hamstrings, quadriceps, and cardiac muscles at 4 weeks after injection. SOD1 mRNA expression is significantly inhibited in cardiac and hamstring muscles. Data are presented as the mean with SD ($n = 4$ for each group, $p < 0.05$ only in the hamstring and heart). (C) The SOD1 protein was also reduced in cardiac and hamstring muscles but not in the liver, as assessed by Western blotting analysis at 4 weeks after injection.

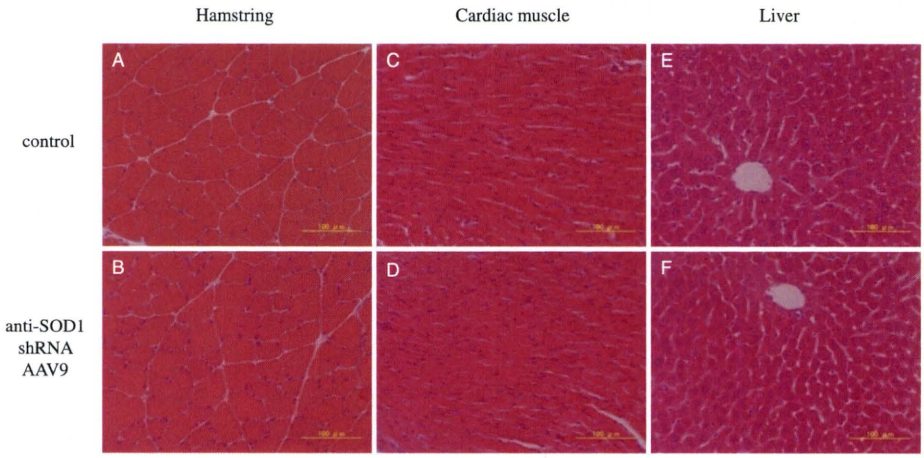


**Fig. 4.** Pathological examination. Photomicrographs of hematoxylin and eosin staining show no abnormalities in the hamstring (A and B), the cardiac muscle (C and D), and the liver (E and F). There were no alterations of cell size or shape, or infiltration of inflammatory cells in both of the groups (scale bar: 100 μm).

**Table 1**
Blood chemistry examinations.

| Group | AST (IU/L) | ALT (IU/L) | ALP (IU/L) | LDH (IU/L) | CK (IU/L) | ALB (g/dL) | TP (g/dL) |
|---|---|---|---|---|---|---|---|
| Control | 36 ± 7 | 16.8 ± 2.2 | 275.8 ± 65.3 | 574.5 ± 60.3 | 143.8 ± 29.9 | 1.7 ± 0.1 | 2.5 ± 0.2 |
| Anti-SOD1 shRNA AAV9 | 56 ± 22.1 | 25.3 ± 11.2 | 273.8 ± 62.8 | 649.3 ± 237.1 | 215.8 ± 121.9 | 1.8 ± 0.1 | 2.6 ± 0.1 |

Mouse body weights were measured 4 weeks after anti-SOD1 shRNA AAV9 vector intraperitoneal injection. Alanine aminotransferase (ALT), aspartate aminotransferase (AST), alkaline phosphatase (ALP), lactate dehydrogenase (LDH), albumin (ALB), serum total protein (TP), creatine kinase (CK). The values are shown as mean ± SD ($n = 4$ in each group, the data of these examinations showed no significant differences between the anti-SOD1 shRNA AAV9 injected mouse group and the littermate control group, $p > 0.05$).

slightly in the anti-SOD1 shRNA AAV9-injected mouse group compared to that in the control littermate group. However, the values in the injected group were within the normal range, and this slight increase was not significant when compared with the littermate control group. Furthermore, serum CK level was also not significantly increased in the injected mice group. These data show that the injected mice could grow and develop without any side effects of the anti-SOD1 shRNA AAV9 vector.

## 4. Discussion

We report that systemic injection of shRNA AAV can inhibit target gene expression in skeletal and cardiac muscle without any adverse side effects. Previous reports state that AAV1, 6, 7, 8 and 9 can deliver specified genes efficiently to skeletal and cardiac muscle [7–10]. However, there is only one report showing significant inhibition in muscles by systemic injection of the shRNA AAV type

6 vector [12]. One explanation for the difficulty with reducing target gene expression in skeletal muscles is liver toxicity of high-dose shRNA as it potentially interferes with the miRNA system [1,4]. Thus, a sufficient dose of shRNA-AAV to effectively reduce target gene expression in skeletal muscles has not been administered, and in previous reports there has been no detailed description about liver dysfunction. The expression of shRNA is reportedly much higher in the liver than in any other tissues; however, shRNA efficacy in the liver is lower than in skeletal muscles [12], which implies the possibility of liver dysfunction. In this study, we effectively reduced our target gene in skeletal muscles by using neonatal mice. In contrast to the previous reports, in our study, northern blot analysis demonstrated almost no expression of shRNA in the liver, which explained the normal liver function that we saw in our mice. Though the mechanism for escaping liver toxicity is not well documented, a few reports have discussed that in neonates the high transduction efficiency in the liver is followed by rapid degradation during liver growth and cell division [9,15]. Our results of high reduction in hamstring muscle but low reduction in liver also indicate that the difference of the dividing or non-dividing characteristic of tissues could influence the efficacy of shRNA AAV in neonates.

Moreover, to evaluate liver function, we included two additional examinations. The first examination was a blood chemical evaluation measuring serum AST, ALT, etc. We found slightly increased serum AST, ALT and LDH in the injected mice; however, these values were within the normal range and were not statistically significant in comparison with the values of the littermate control group. The second examination was liver pathology. We found no morphological liver abnormalities such as swelling or atrophy, and could not find any inflammatory changes or destruction of hepatic lobules, microscopically. From these evaluations, we concluded that intraperitoneal injection of shRNA AAV into neonates does not induce any liver dysfunction.

We noted a difference in the expressed level of siRNA and the reduction rate of SOD1 gene between hamstring muscles and quadricep muscles. A few reports have discussed the difference in efficacy of AAV-delivered gene transduction among the skeletal muscles [6,9,10,15,19], but the reasons behind this remained uncertain. We believe that some of the reasons are as follows: different fiber type; the expression rate for AAV receptors may be different in each muscle; the pathway of systemic AAV circulation might affect the delivery; and the characteristics of U6 promoters might influence the AAV-delivered gene transduction in skeletal muscles.

Some studies discuss the relationship between AAV transduction and muscle fiber typing [6,15,19]; however, our results did not show such a correlation (data not shown). Considering AAV circulation, one report describes the correlation between the silencing effects and capillary density in the skeletal muscles, whereby the authors concluded that AAV circulation might not affect the difference seen among skeletal muscles [10]. AAV receptors have not yet been clearly identified. One of the receptors, the laminin receptor, has been analyzed in skeletal muscle, but the difference in the muscles was unaffected by this receptor alone [10]. Further studies are necessary to clarify the mechanisms behind the difference of gene targeting in muscle tissues, with one way to resolve this problem being the generation of systemic skeletal muscle disease animal models using the method described in this study.

We consider that the method used in this study offers a novel way to generate conditional knockdown in vivo models in certain skeletal and cardiac muscle tissue diseases. In particular, in some causative gene knockout models, it is very difficult to establish embryonic lethality, such as with the UDP-*N*-acetylglucosamine 2-epimerase/*N*-acetylmannosamine kinase (GNE) gene in distal myopathy with rimmed vacuoles (DMRV)/hereditary inclusion body myopathy (hIBM) [20,21], and Angiopoietin-1 gene related to prominent defects in endocardial and myocardial development [22]. To circumvent this limitation, reducing the target protein after birth might be a very powerful method for generating conditional knockdown models. In this study, we effectively reduced SOD1 gene expression in skeletal muscles, without any muscle damage. During the entire growth course of the mice, we did not observe growth retardation, abnormal motor ability, signs of heart or hepatic failures, or abnormal biochemical and pathological findings that would indicate the degeneration of skeletal and cardiac muscles in these injected mice. These results suggest that this shRNA AAV intraperitoneal injection method may not involve the liver, thus allowing us to examine the knockdown effects of our target gene in skeletal and cardiac muscles specifically.

Although we confirmed the gene-silencing effect in the muscles up to 2 months (data not shown), we did not examine how long the silencing effect would potentially last. It has been reported that shRNA transgenic mice with the same shRNA used in this study showed marked suppression of SOD1 for more than 1 year [3]. However, protein expressed by systemically injected AAV has been reported to reduce in humans within months, probably due to immunological elimination by CD8 memory T cells [23]. Although we considered there to be no memory CD8 T cells in our system because we injected the AAV just 1 day after birth, we still need to confirm the duration of the silencing effect.

Finally, we need to confirm the long-term safety of AAV and shRNA. Since the transduction or reduction of the target genes systemically is a very attractive method of gene therapy in skeletal muscle disease, this delivery system is useful not only for generating knockdown mouse models, but also for gene therapy of congenital cardiac and skeletal muscle disease.

## Acknowledgments

This study was supported by the Research Grant (20B-13) for Nervous and Mental Disorders from the Ministry of Health, Labour and Welfare.

## References

[1] J.J. Rossi, Expression strategies for short hairpin RNA interference triggers, Hum. Gene Ther. 19 (2008) 313–317.
[2] X. Gao, P. Zhang, Transgenic RNA interference in mice, Physiology 22 (2007) 161–166.
[3] Y. Saito, T. Yokota, T. Mitani, K. Ito, M. Anzai, M. Miyagishi, K. Taira, H. Mizusawa, Transgenic small interfering RNA halts amyotrophic lateral sclerosis in a mouse model, J. Biol. Chem. 52 (2005) 42826–42830.
[4] D. Grimm, K.L. Streetz, C.L. Jopling, T.A. Storm, K. Pandey, C.R. Davis, P. Marion, F. Salazar, M.A. Kay, Fatality in mice due to oversaturation of cellular microRNA/short hairpin RNA pathways, Nature 25 (2006) 537–541.
[5] T.R. Magee, J.N. Artaza, M.G. Ferrni, D. Vermet, F.I. Zuniga, L. Cantini, S. Reisz-Porszasz, J. Rajfer, N.F. Gonzalez-Cadavidm, Myostatin short interfering hairpin RNA gene transfer increases skeletal muscle mass, J. Gene Med. 8 (2006) 1171–1181.
[6] J.P. Louboutin, L. Wang, J.M. Wilson, Gene transfer into skeletal muscle using novel AAV serotypes, J. Gene Med. 7 (2005) 442–451.
[7] C. Zincarelli, S. Soltys, G. Rengo, J.E. Rabinowitz, Analysis of AAV serotypes 1–9 mediated gene expression and tropism in mice after systemic injection, Mol. Ther. 16 (2008) 1073–1080.
[8] M.J. Blankinship, P. Gregorevic, J.M. Allen, S.Q. Harper, H. Harper, C.L. Halbert, A.D. Miller, J.S. Chamberlain, Efficient transduction of skeletal muscle using vectors based on adeno-associated virus serotype 6, Mol. Ther. 10 (2004) 671–678.
[9] Z. Wang, T. Zhu, C. Qiao, L. Zhou, B. Wang, J. Zhang, C. Chen, J. Li, X. Xiao, Adeno-associated virus serotype 8 efficiently delivers genes to muscle and heart, Nat. Biotechnol. 23 (2005) 321–328.
[10] Y. Yue, A. Ghosh, C. Long, B. Bostick, B.F. Smith, J.N. Komegay, D.A. Duan, A single intravenous injection of adeno-associated virus serotype-9 leads to whole body skeletal muscle transduction in dogs, Mol. Ther. 16 (2008) 1944–1952.
[11] K. Inagaki, S. Fuess, T.A. Strom, G.A. Gibson, C.F. Mctiernan, M.A. Kay, H. Nakai, Robust systemic transduction with AAV9 vectors in mice: efficient global cardiac gene transfer superior to that of AAV8, Mol. Ther. 14 (2006) 45–53.

[12] C. Towne, C. Raoul, B.L. Schneider, P. Aebischer, Systemic AAV6 delivery mediating RNA interference against SOD1: neuromuscular transduction does not alter disease progression in fALS mice, Mol. Ther. 16 (2008) 1018–1025.
[13] T. Ogura, H. Mizukami, J. Mimuro, S. Madoiwa, T. Okada, T. Matsushita, M. Urabe, A. Kume, H. Hamada, H. Yoshikawa, Y. Sakata, K. Ozawa, Utility of intraperitoneal administration as a route of AAV serotype 5 vector-mediated neonatal gene transfer, J. Gene Med. 8 (2006) 990–997.
[14] K.D. Foust, A. Poirier, C.A. Pacak, R.J. Mandel, T.R. Flotte, Neonatal intraperitoneal or intravenous injection of recombinant adeno-associated virus type 8 transduce dorsal root ganglia and lower motor neurons, Hum. Gene Ther. 19 (2008) 61–70.
[15] B. Bostick, A. Ghosh, Y. Yue, C. Long, D. Duan, Systemic AAV-9 transduction in mice is influenced by animal age but not by the route of administration, Gene Ther. 14 (2007) 1605–1609.
[16] K.D. Foust, E. Nurre, C.L. Montgomery, A. Hernandez, C.M. Chen, B.K. Kaspar, Intravascular AAV9 preferentially targets neonatal neurons and adult astrocytes, Nat. Biotechnol. 27 (2009) 59–65.
[17] T. Yokota, M. Miyagishi, T. Hino, R. Matsumura, A. Tasinato, M. Urushitani, R.V. Rao, R. Takahashi, D.E. Bredesen, K. Taira, H. Mizusawa, SiRNA-based inhibition specific for mutant SOD1 with single nucleotide alternation in familial ALS, compared with ribozyme and DNA enzyme, Biochem. Biophys. Res. Commun. 314 (2004) 283–291.
[18] W.T. Hermens, O. Ter Brake, P.A. Dijkhuizen, M.A. Sonnemans, D. Grimm, J.A. Kleinschmidt, J. Verhaagen, Purification of recombinant adeno-associated virus by iodixanol gradient ultracentrifugation allows rapid and reproducible preparation of vector stocks for gene transfer in nervous system, Hum. Gene Ther. 10 (1999) 1885–1891.
[19] C.A. Pacak, T. Conlon, C.S. Mah, B.J. Byme, Relative persistence of AAV serotype 1 vector genomes in dystrophic muscle, Genet. Vaccines Ther. 6 (2008) 14.
[20] M. Schwarzkopf, K.P. Knobeloch, E. Rohde, S. Hinderlich, N. Wiechens, L. Lucka, I. Horak, W. Reutter, R. Horstkorte, Sialylation is essential for early development in mice, Proc. Natl. Acad. Sci. USA 99 (2002) 5267–5270.
[21] M.C. Malicdan, S. Noguchi, I. Nonaka, Y. Hayashi, I. Nishino, A Gne knockout mouse expressing human GNE D176V mutation develops features similar to distal myopathy with rimmed vacuoles or hereditary inclusion body myopathy, Hum. Mol. Genet. 16 (2007) 2669–2682.
[22] C. Suri, P.F. Jones, S. Patan, S. Bartunkova, P.C. Maisonpierre, S. Davis, T.N. Sato, G.D. Yancopoulos, Requisite role of angiopoietin-1, a ligand for the TIE2 receptor, during embryonic angiogenesis, Cell 87 (1996) 1171–1180.
[23] C.S. Manno, G.F. Pierce, V.R. Arruda, B. Glader, M. Ragni, J.J. Rasko, M.C. Ozelo, K. Hoots, P. Blatt, B. Konkle, M. Dake, R. Kaye, M. Razavi, A. Zajko, J. Zehnder, P.K. Rustagi, H. Nakai, A. Chew, D. Leonard, J.F. Wright, R.R. Lessard, J.M. Sommer, M. Tigges, D. Sabatino, A. Luk, H. Jiang, F. Mingozzi, L. Couto, H.C. Ertl, K.A. High, M.A. Kay, Successful transduction of liver in hemophilia by AAV-Factor IX and limitations imposed by the host immune response, Nat. Med. 12 (2006) 342–347.

HUMAN GENE THERAPY 22:27–34 (January 2011)

DOI: 10.1089/hum.2010.054

**Research Articles**

# *In Vivo* Application of an RNAi Strategy for the Selective Suppression of a Mutant Allele

Takayuki Kubodera,[1] Hiromi Yamada,[1] Masayuki Anzai,[2] Shinga Ohira,[1] Shigefumi Yokota,[1] Yukihiko Hirai,[3] Hideki Mochizuki,[4] Takashi Shimada,[3] Tasuku Mitani,[2] Hidehiro Mizusawa,[1] and Takanori Yokota[1]

**Abstract**

Gene therapy for dominantly inherited diseases with small interfering RNA (siRNA) requires mutant allele-specific suppression when genes in which mutation causes disease normally have an important role. We previously proposed a strategy for selective suppression of mutant alleles; both mutant and wild-type alleles are inhibited by most effective siRNA, and wild-type protein is restored using mRNA mutated to be resistant to the siRNA. Here, to prove the principle of this strategy *in vivo*, we applied it to our previously reported anti–copper/zinc superoxide dismutase (SOD1) short hairpin RNA (shRNA) transgenic (Tg) mice, in which the expression of the endogenous wild-type *SOD1* gene was inhibited by more than 80%. These shRNA Tg mice showed hepatic lipid accumulation with mild liver dysfunction due to downregulation of endogenous wild-type SOD1. To rescue this side effect, we generated siRNA-resistant SOD1 Tg mice and crossed them with anti-SOD1 shRNA Tg mice, resulting in the disappearance of lipid accumulation in the liver. Furthermore, we also succeeded in mutant SOD1-specific gene suppression in the liver of $SOD1^{G93A}$ Tg mice, a model for amyotrophic lateral sclerosis, using intravenously administered viral vectors. Our method may prove useful for siRNA-based gene therapy for dominantly inherited diseases.

## Introduction

RNA INTERFERENCE (RNAi) is evolutionally conserved sequence-specific post-transcriptional gene silencing mediated by small double-stranded RNA (Elbashir *et al.*, 2001). This post-transcriptional gene silencing can be effectively induced by exogenously introduced small interfering RNA (siRNA) or intracellularly expressed short hairpin RNA (shRNA) in mammalian cells (Dykxhoorn *et al.*, 2006a). The therapeutic efficacy of RNAi on human diseases has been demonstrated in various animal models using either directly delivered siRNA or viral vector-delivered shRNA (Bumcrot *et al.*, 2006; Kim and Rossi, 2007). Among the promising targets for siRNA/shRNA therapy are dominantly inherited diseases in which the aberrant proteins encoded by mutant alleles are eliminated by siRNA/shRNA. In order to test the hypothesis that siRNA-mediated mutant gene silencing is able to ameliorate dominantly inherited diseases, we generated shRNA transgenic (Tg) mice in which shRNA against copper/zinc superoxide dismutase (SOD1) was ubiquitously overexpressed. This mouse demonstrated marked suppression of endogenous *SOD1*, the gene in which mutation causes familial amyotrophic lateral sclerosis (ALS) (Saito *et al.*, 2005; Yokota *et al.*, 2007). When $SOD1^{G93A}$ Tg mice, a model for ALS (Gurney *et al.*, 1994), were crossed with anti-SOD1 shRNA Tg mice, the resultant double Tg mice demonstrated a dramatic delay in the onset and progression of ALS by inhibiting mutant SOD1 production (Saito *et al.*, 2005; Yokota *et al.*, 2007).

A major problem encountered in our strategy to silence the mutant allele with RNAi in $SOD1^{G93A}$ Tg mice was that expressed siRNA failed to specifically recognize the point mutation, resulting in suppression of the wild-type allele in addition to the mutant allele. In order to treat dominantly inherited diseases using this RNAi strategy, mutant allele-specific suppression is necessary, especially when the genes in which mutation causes diseases have normally an important role. Anti-SOD1 shRNA Tg mice that demonstrate marked

[1]Department of Neurology and Neurological Science, Tokyo Medical and Dental University, Bunkyo-ku, Tokyo 113-8519, Japan.
[2]Institute of Advanced Technology, Kinki University, Kainan, Wakayama 642-0017, Japan.
[3]Department of Biochemistry and Molecular Biology, Nippon Medical School, Bunkyo-ku, Tokyo 113-8602, Japan.
[4]Department of Neurology, School of Medicine, Kitasato University, Sagamihara, Kanagawa 252-0374, Japan.

suppression of endogenous wild-type SOD1 also exhibit a fatty liver, similar to that observed in SOD1 knockout mice (Sasaguri *et al.*, 2009). siRNA can be designed to discriminate between single nucleotide alterations by targeting the mutation itself or disease-linked polymorphisms (Gonzalez-Alegre *et al.*, 2003; Miller *et al.*, 2003, 2004; Li *et al.*, 2004; Dykxhoorn *et al.*, 2006b; van Bilsen *et al.*, 2008). In a systematic analysis investigating the design of single nucleotide-specific siRNA, mismatches located in the central and 3′ regions of the guide strand (especially at positions 10 and 16 from the 5′ end) provided a high efficacy of single nucleotide discrimination between mutant and wild-type alleles (Schwarz *et al.*, 2006). Introducing a mismatch into the seed region of siRNA was also shown to enhance discrimination (Ohnishi *et al.*, 2008). We have also reported on the design of siRNA that demonstrates relative discrimination of a mutant allele possibly resulting from a change in the RNA secondary structure (Li *et al.*, 2004).

Despite these design strategies, discrimination of mutant and wild-type alleles is not always complete. In addition, the cleavage efficiency of the mutant allele is not necessarily maximal, as the selection sites used in the design of siRNA are limited to the siRNA-related region. More than 125 different mutations in the *SOD1* gene in familial ALS have been identified to date (Pasinelli and Brown, 2006). We have designed mutant allele-specific siRNA for G93A and A4V SOD1 (Yokota *et al.*, 2004), but not for G37R SOD1. To overcome these problems, we proposed a novel method for allele-specific suppression by siRNA where both mutant and wild-type alleles are inhibited by most effective siRNA and where wild-type protein is restored using wild-type mRNA modified to be resistant to the siRNA. The amino acid sequence encoded by modified mRNA is the same as that of native mRNA, whereas the nucleotide sequence of mRNA targeted by siRNA is altered (Kubodera *et al.*, 2005). A similar method of mutant allele-specific siRNA design was reported by another group in the same year (Xia *et al.*, 2005). Here, we examined this strategy *in vivo* by applying the method to the rescue of the anti-SOD1 shRNA Tg mice phenotype and to the selective suppression of the mutant allele in $SOD1^{G93A}$ Tg mice.

## Materials and Methods

### *Construction of expression vectors*

Construction of anti-SOD1 shRNA expression vector has been reported previously (Saito *et al.*, 2005). The shRNA sequence (sense sequence position 536–555, NM_000454) of this vector was common to the siRNA target region in both human and mouse SOD1 mRNA. siRNA-resistant human SOD1 expression vector, in which the human wild-type SOD1 genome is mutated so that it is not cleaved by the anti-SOD1 siRNA but is translated to the same amino acid sequence of native human SOD1, was made by site-directed mutagenesis (Stratagene, La Jolla, CA). The human SOD1 promoter and wild-type SOD1 genomic DNA were kindly provided by Dr. Masashi Aoki.

For recombinant adeno-associated virus (rAAV)-mediated delivery of shRNA targeting SOD1 and siRNA-resistant mouse SOD1 cDNA, the anti-SOD1 shRNA expression cassette containing human U6 promoter (shRNA) or that followed by the siRNA-resistant mouse SOD1 expression cassette containing cytomegalovirus (CMV) promoter (siRNA-resistant) was cloned into the plasmid containing adeno-associated virus (AAV) serotype 2 inverted terminal repeats (pAAV-MCS) (Stratagene). For genome copy titration of rAAV vectors, the human growth hormone poly(A) signal was inserted downstream of the shRNA cassette.

### *Viral vector production*

The rAAV pseudotyped-8 (rAAV-2/8; AAV-2 inverted terminal repeat, AAV-8 viral capsid) vectors were produced using the adenovirus-free triple transfection method (Stratagene). The AAV vector plasmid (pAAV), the packaging plasmid (P5E18-VD2/8; a gift from Dr. James M. Wilson, University of Pennsylvania, Philadelphia, PA), and a helper plasmid (pHelper; Stratagene) were co-transfected into human embryonic kidney 293 cells under calcium phosphate precipitation. At 6 hr after transfection, the culture medium was replaced with fresh medium, and the cells were incubated for 48 hr. The cells were then harvested from the culture dishes and pelleted by centrifugation, resuspended in phosphate-buffered saline (PBS), and subjected to three rounds of freeze–thawing. Cell debris was then pelleted by centrifugation at 1,200*g* for 15 min. AAV vectors were purified using ammonium sulfate precipitation and iodixanol (Axis-Shield, Norton, MA) continuous gradient centrifugation. Genome titers of the AAV vectors were determined by quantitative polymerase chain reaction (PCR) using the TaqMan system (Taymans *et al.*, 2007). The following primers and probes targeting the poly(A) signal were used: 5′-CAGGCTGGTC TCCAACTCCTC-3′ and 5′-GCAGTGGTTCACGCCTGTAA-3′ served as the primer set, and 5′-TACCCACCTTGGCCTC-3′ served as the probe.

### *Animals*

Animal experiments were performed in accordance with the Guidelines for Animal Experimentation of Tokyo Medical and Dental University and were pre-approved by the local ethics committee (protocol 0090104). The generation of anti-SOD1 siRNA Tg mice has been described previously (Saito *et al.*, 2005). To produce siRNA-resistant human SOD1 Tg mice, the siRNA-resistant human SOD1 expression vector was injected into fertilized mouse eggs. Double Tg mice were generated by crossing anti-SOD1 shRNA Tg mice with siRNA-resistant human SOD1 Tg mice. Genotypes of the mice were determined by PCR analysis using genomic DNA from the tail tip. PCR was carried out using the following primer sets: 5′-CATCAGCCCTAATCCATCTGA-3′ and 5′-CGCGACTAACAATCAAAGTGA-3′ for siRNA-resistant human SOD1 Tg mice and 5′-CTTGGGTAGTTTGCAG-3′ and 5′-CAGGAAACAGCTATGAC-3′ for anti-SOD1 shRNA Tg mice.

### *AAV injection*

$SOD1^{G93A}$ Tg mice were intravenously administered a single dose of $1\times10^{12}$ vector genomes of rAAV2/8-shRNA or -shRNA/resistant SOD1 vectors via the tail vein. All mice were sacrificed 3 weeks post-injection. Mice were deeply anesthetized with pentobarbital sodium and perfused with cold PBS. Tissue samples were then collected and snap-frozen in liquid nitrogen for analysis.